The kinetics of gypsum precipitation, the inhibiting effect of citric acid and its use in the differential precipitation of $Mg(OH)_2$ from $CaSO_4 \cdot 2H_2O$

PhD dissertation

Szilveszter Ziegenheim

Supervisors:
Prof. Dr. Pál Sipos
Prof. Dr. István Pálinkó

Doctoral School of Environmental Sciences
Material and Solution Structure Research Group
Department of Inorganic and Analytical Chemistry
Faculty of Science and Informatics | University of Szeged

Szeged
2021

Table of contents

1. Introduction

The crystallization of solids from supersaturated solutions is a source of numerous complications during a range of industrial processes: undesirable precipitates may clog pipelines, foul membranes, contaminate the target compounds of a process, lower the effectiveness of heat-exchange *via* scale formation, *etc*. Calcium sulfate dihydrate ($CaSO_4 \cdot 2H_2O$ or gypsum) is one of the most common of such solids, therefore during the last decades, numerous studies were dedicated to the investigation of the precipitation kinetics and method development potentially suitable for precipitation control and inhibition.

In the experimental work leading to this dissertation, the kinetics of gypsum precipitation was studied in the entire experimentally available concentration range. The impact of citric acid (or citrate ion) on the reaction was investigated in detail including some experiments in unconventional media. The acquired experience was used to optimize the differential precipitation of magnesium hydroxide from gypsum, which provides a promising method to improve the treatments of acidic wastewaters economically and in environmentally friendly way, and could also be useful in desalination processes.

2. Literature review

2.1. Crystallization

The process when atoms or molecules are arranged to a well-defined, organized solid structure is called crystallization. The common ways of crystallization are freezing and precipitation from solutions, but in some rare cases, solids can be deposited directly from gases. These processes can occur naturally or can be induced artificially, and they can be influenced by a number of factors, for example temperature, chemical composition and agitation, *etc*. Various products of crystallization can be found in our everyday lives. The scales in the bathtub, the sea salt made by evaporation process and the crystalline form of cocoa butter, chocolate that is, are all resulted from some way of crystallization. During the last decades, a considerable number of textbooks were dedicated to summarize the rapidly expanding body of knowledge acquired in this field, see refs. [1-4], without claiming that the list is complete. Since the primary focus of this work is concerned with precipitation processes, first they will be discussed in detail.

2.1.1. Solubility and Supersaturation

Solutions are homogeneous systems consisting of two or more compounds, which are usually called solute(s) and solvent(s). The most commonly used solvent is water, it is practically the only solvent used in the industrial scale crystallization of inorganic substances. Solubility determines the capability of a solute (solid, liquid or gas) to be dissolved in a given solvent under well-specified conditions. The solubility is highly dependent on the temperature and the chemical composition of the solute and solvent, but other substances present in the system can also influence it. It is usually tabulated in terms of the molar concentration of the saturated solution; however, for ionic species it can be better described using the activity of the dissolved ions. This activity is given as the product of the activity coefficient (γ) and the molar concentration. The limitations regarding the activity coefficient of dissolved ionic species are given by the Debye-Hückel equation:

$$\log \gamma_{\pm} = -A|z_{+}z_{-}|I^{1/2} \quad (1)$$

where A is the temperature-dependent Debye-Hückel constant, z_+ and z_- are the valencies of the cations and anions, respectively, and I is the ionic strength. The latter can be defined as:

$$I = \frac{1}{2}\sum c_i z_i^2 \quad (2)$$

where c_i is the molar concentration (mol/L) of the *i*th species and z_i is the valency of that ion.

This approximation is only reliable in infinitely dilute systems, in solutions with higher ionic strength other considerations must be made. Using the Davies equation [5]

$$\log \gamma_{\pm} = -A|z_+ z_-| \left\{ \left[\frac{I^{\frac{1}{2}}}{I + I^{\frac{1}{2}}} \right] - 0.3I \right\} \quad (3)$$

the activity of dissolved ionic species can be soundly described up to 0.2 M ionic strength. For solutions with higher ionic strengths, further considerations must be made.

When thermodynamic equilibrium is reached between the solution and solid phase at the given temperature, we are talking about saturated solutions. Sometimes; however, it is possible to make more concentrated solutions, for example by slowly cooling a saturated solution without agitation, resulting in a supersaturated solution.

Having a supersaturated solution is a necessity for every crystallization process; however, the state of supersaturation does not guarantee that spontaneous nucleation will take place. This phenomenon is best represented with a solubility-supersolubility diagram, as seen in Figure 1.

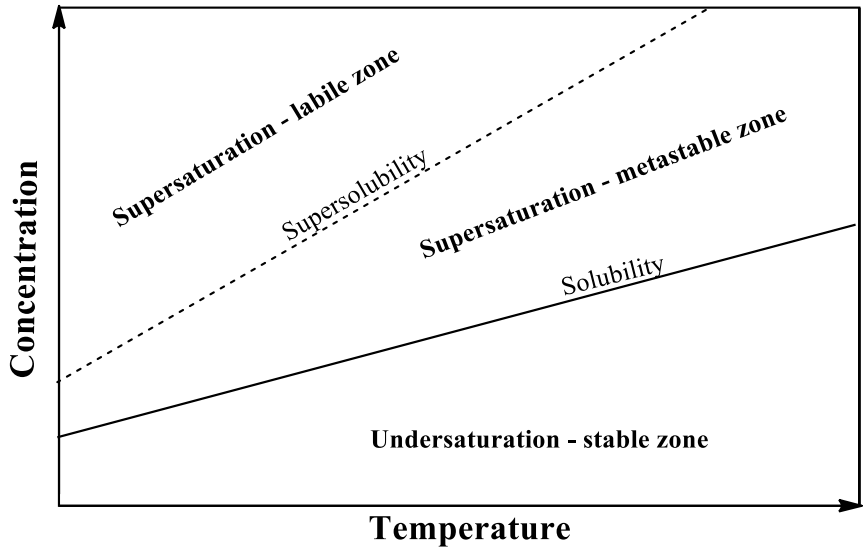

Figure 1. Schematic representation of solubility-supersolubility diagram

Research focusing at the connection between supersaturation and nucleation (the formation of solid nuclei, that is, see section 2.1.2) showed that in solutions with moderate supersaturation, crystallization is improbable to occur, unless induced artificially; they are in a metastable state. The experimental conditions exert a big impact on the width of the metastable zone; agitation, rate of the concentration increase, and the presence of impurities and additives – all of these are strongly influential parameters. Increasing the supersaturation

will move the solution into labile state, where the precipitation is very likely to occur spontaneously [6].

In systems with slow nucleation, the process may take place at moderate, constant supersaturation. In these cases, the nucleation rate is described with induction time, the time necessary for the formation of nuclei with (experimentally) observable size.

2.1.2. Nucleation

Before well-formed crystals can develop, miniature particles – they are called embryos, nuclei, seeds – must be present in the solution to act as centers of crystallization. Nucleation can be induced by multiple means, such as agitation, friction, mechanical shock *etc.* [7]. Nucleation can be classified as primary or secondary nucleation. When primary nucleation takes place without any solids present in the solution, then it is called homogenous nucleation. When it is induced by some foreign solids it is called heterogeneous nucleation. Secondary nucleation occurs, irrespectively of its mechanism, when crystals of the material are already present in the crystallizing system forming new crystallization centers by fragmentation [4] (see also section 2.2).

The exact mechanism of homogenous nucleation is still not fully understood, since the dimension where the process takes place is too small to be directly observed, but still many researchers tried to describe the process in detail. In most cases, the basis of nucleation theories is the condensation of vapors to liquid. They are very similar to a point, as in both cases, minute particles are formed, capable of redissolving despite the supersaturation of their environment. Furthermore, in crystallization, more than the "simple" aggregation of the nuclei is necessary: they must be aggregated in the right order and orientation to form crystals. The precipitation will only proceed if these crystals reach the critical size and structure needed, thus, they could act as crystallization centers [1-3].

The alternative way of nucleation to occur is the so-called heterogeneous nucleation. The rate of nucleation can be significantly modified by even trace amounts of added nuclei (seeding) or impurities present in or deliberately added to the system. General rules cannot be applied, a successful inhibitor/seed in one case may not work in another, every situation must be considered separately. The nucleation of a crystallizing system can be induced by the presence of crystalline impurities acting as active particles, "heteronuclei" [2]. In a lot of cases, homogeneous nucleation is actually induced by heterogeneous crystal impurities. Some people say that homogenous nucleation cannot happen, as even the most carefully

prepared solutions contain some residual minuscule particles, and they are inducing the crystallization [1].

The concept of nucleation kinetics is even more complicated if the secondary nucleation is taken into consideration. From the surface of the primarily formed crystals smaller particles can be torn by either collision of the crystals or by the shearing forces of the solution caused by agitation or turbulence. These tiny particles can also act as new nucleus, thus enhancing the rate of crystallization.

2.1.3. Crystal growth

When the nuclei reach the critical size, they become stable and will not be redissolved, but continue to grow. There are various mechanisms proposed to describe the growth of crystals.

Surface energy theory suggests that crystals tend to grow on points/lattices with the least surface energy, as they should grow to a shape with minimal surface energy. The different faces of the crystals have diverse surface energy, and, therefore will grow at different rates. As a result, most of the crystals will not maintain their geometric form during growth, the smaller, quickly growing sites may disappear. This mode of crystal growth is called "overlapping" [8]. The main shortcoming of the theory is that it cannot explain the effect of supersaturation and solution movement on the rate of crystal growth.

The *adsorption layer theory* states that the solute compounds, to get to the growth site from the bulk solution, move in an interfacial film of solute, adsorbed on the surface of the crystals. According to this theory, the solute particles reaching the crystal surface are not immediately built in the lattices, but can migrate through surface diffusion to the active centers, where the attractive forces are the strongest. This step-by-step growth will continue, until the growing layer is complete. For a new layer to grow, a new site of growth must be formed on the present layers' surface. Beside crystal growth, the transition phase can play a large role in the secondary nucleation as well. Of course, the layers are not growing in strict order, they always have some flaws, and the new layers can start growing before the expansion of the upholding layer is finished [2]. Kossel's model depicts the concept; the scheme is presented in Figure 2.

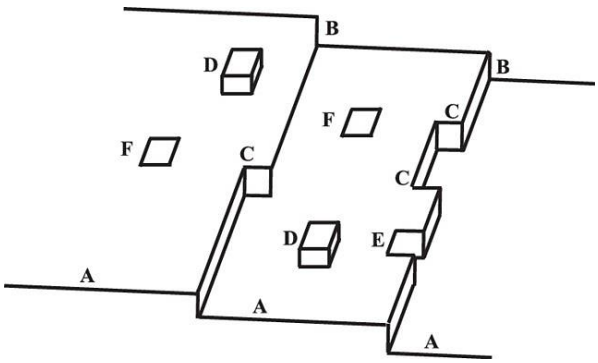

Figure 2. Kossel's model of growing crystal surfaces A: flat layers B: steps C: kinks D: surface adsorbed growth units E: edge vacancies, F: surface vacancies [2]

The model works well in solutions with high supersaturation, but since the surface nucleation is unlikely to occur at low or moderate supersaturation, it does not work well for those systems. The solution for this shortcoming came from Frank [9] suggesting that crystals rarely grow smoothly layer-by-layer, but rather have dislocations around the sites. This can neglect the need for surface nucleation, once a screw dislocation is formed, the solid can continuously grow in a spiral. Burton, Cabrera and Frank developed the model further, and were able to calculate the growth rate of crystals growing from vapors at any supersaturation [10]. The application of this model on solutions is more difficult because of the varying viscosities and diffusivities and the large changes in ion-mobilities and hydration characteristics during the process. *Kinematic theory* goes one step further and considers thicker (multiatomic) layers with uneven distribution taking into account two growth steps, the formation of new layers/steps and their "movement" by growth [11]. *Birth and spread* (or nuclei on nuclei) theory describes crystal growth with surface nucleation followed by the spread of the layer [12].

The *diffusion-reaction theory* is based on the concept that dissolution and crystallization are reverse processes, and they are driven by the differences in concentration at the solid surface and in the bulk of the solution. The assumption of a stagnant surface fluid layer on the crystals and that this fluid is still supersaturated lead to the suggestion that the solute is built in the crystal in two steps. First it gets to the solid surface from the bulk by a diffusion process, then they are arranged to the structure through a first order reaction [1, 2]. Realistically, the mechanism of crystal growth cannot be described with only one of these theories, rather multiple processes are involved.

The rate of the crystal growth is affected by several external factor, but most importantly by the supersaturation. As the main driving force of crystallization, it naturally effects the

growth rate, but it can influence the morphology and homogeneity of the crystals. At low supersaturation, the growth rate of layers can be balanced resulting in crystals with evenly developed faces. With the increasing supersaturation, some faces may grow faster than the others, therefore the crystals will not grow uniformly in every direction. At high supersaturation it is also possible that a newer layer is closed sooner than the previously formed ones resulting in the inclusion of the mother liquor in the solid.

Another very important factor is the temperature. Similarly to every other chemical reaction, it affects the kinetics of the crystallization in many ways. Increased temperature can decrease the activation energy needed for primary nucleation, increases the number of compound collisions, enhances the diffusion rate, affects the hydration of the solute, *etc*. [1, 2]. Beside the effects mentioned above, temperature can influence the crystallization rate indirectly by changing supersaturation rates, since the solubility of solids is highly dependent on temperature. It can even determine the crystal form in which the solid precipitate [13].

Even the size of the crystals can change the growth rate. The smaller crystals, having smaller terminal velocities compared to bigger ones in a fluid, can grow slower in agitated systems. Crystals near the critical nucleation size grow slower due to their higher solubility and therefore smaller supersaturation. Also, bigger crystals statistically must have more dislocations on their surfaces, and due to their bigger size and translational velocity, they will collide with more solute particles.

Last but not least, the effect of impurities must be discussed. These can have diverse effects on crystallization. They can suppress the precipitation entirely, or only modify the growth of some faces, thus changing the morphology. Some are efficient in trace amounts and some need to be present in high quantities. They can change the solubility of the crystallizing compound through changing the rate of supersaturation, or interact with the adsorption layer of the surface of the crystals (Figure 3), thus slowing or stopping the growth of crystal layers. If the foreign compounds are strongly bound to the crystals, they can in principle be even incorporated generating dislocations in the structure. Indeed, the list of the possible impurity effects can further be continued.

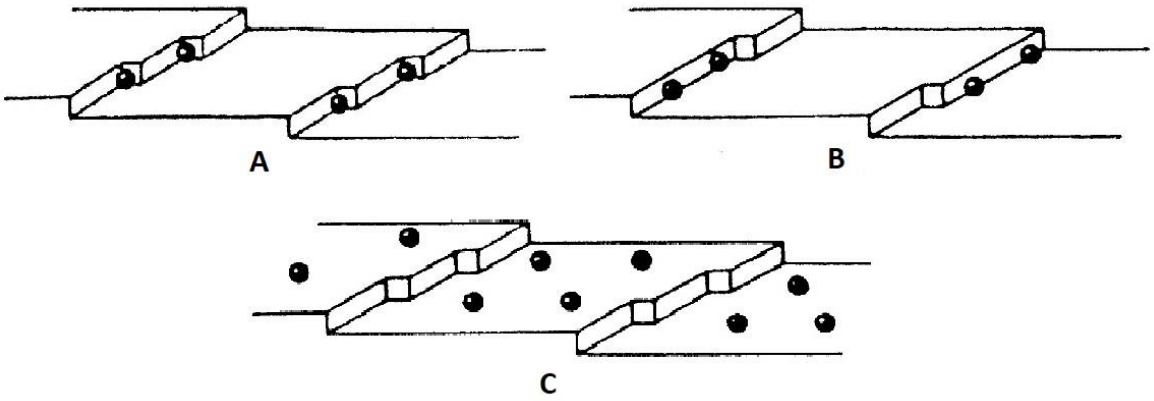

Figure 3. Possible sites for adsorption of impurities on crystal surfaces using Kossel's model A: in kinks B: in front of steps C: on crystal face [2]

Crystallization is a widely used industrial process, but if unwanted, it can cause a lot of nuisances in various processes. Scaling in pipes is a major problem in many processes, because it can decrease the pipe diameter and even clog the system [14-16]. Solid deposition on heat-exchanging surfaces can largely decrease the efficiency of the process, therefore the hindrance of precipitation is a pressing matter in these systems [17-19]. The precipitation of solids from oil-field waters is also an important issue. It can set back the drilling in multiple ways, therefore it is important to know if the mixing of the present and injected water will result in solid deposition [20-22]. Reverse osmosis technique is an efficient solvent-purifying technique often used during industrial processes and for the production of pure water. Scaling and precipitation can dramatically decrease the efficiency of the process; that is why the inhibition of those processes was subject of several studies, for example [23-25]. Among the solids interfering with these processes, calcium sulfate is one of the most common. It crystallizes most often in the form of dihydrate, $CaSO_4 \cdot 2H_2O$, the well-known trivial name of this compound is gypsum. The present PhD work is mostly dedicated to the study of the crystallization of gypsum, to the possibilities of its inhibition and to the potential of finding feasible industrial applications of our results. Therefore, in the following sections we will make an attempt to give an overview on the already established knowledge regarding this topic.

2.2. The precipitation of calcium sulfate dihydrate ($CaSO_4 \cdot 2H_2O$ or gypsum)

Gypsum is present in Nature, and is found in a wide range of industrial processes. Beside the ones mentioned in the previous sections of this dissertation, gypsum precipitates during

phosphonic acid production [26-28], where the quality of the solids is an important factor in the purification of the product. The removal of sulfur-containing gases from flue gas is a serious issue in terms of environmental protection, and such procedures are routinely used worldwide. During the wet process of flue gas desulfurization, which is performed with the use of lime or limestone, one of the crystallizing solids is gypsum [29-31]. Another environmentally important process is the treatment of acidic wastes, such as acidic mine drainages or waste sulfuric acid. These fluids contain sulfate ions in high concentrations, and are usually neutralized by lime or limestone, resulting in solutions supersaturated with respect to calcium sulfate [32-34]. These issues and their clear practical significance are the reasons why the precipitation of gypsum is a widely studied phenomenon even today.

2.2.1 Kinetics of gypsum precipitation

The first experiments investigating the precipitation kinetic of gypsum were made in the late fifties [35, 36]; however, detailed study regarding the topic commenced only during the seventies. To investigate the kinetics of precipitation, both the nucleation and the crystal growth processes must be studied.

The earlier works focused mainly on the crystal growth of gypsum. To experimentally separate the nucleation and growth processes, seeded reaction were carried out by employing small or moderate levels of supersaturation. If sufficient amount of gypsum crystals is added to the solution, the crystals will grow, and the effect of secondary nucleation on the kinetics will be expected to be negligible. If the amount of seeds is decreased or the supersaturation is increased, the signs of secondary nucleation will become observable [37].

Over the next two decades several works were dedicated to this particular field. The authors executed seeded experiments at low supersaturation, similar to the early studies. Here, the effect of temperature was investigated in a wide range, to determine the growth rate and the activation energy of the process, and to investigate the possible phase-transition of dihydrate to hemihydrate or anhydrate [37, 38]. The growth of gypsum was studied in similar experiments at constant (room) temperature and at small supersaturation, to describe the growth process and investigate the effect of the preparation history of the seeds [39-41]. The influence of NaCl on the crystal growth was also studied [42]. In most cases, stable supersaturated solutions were prepared by dissolving the more soluble hemihydrate in distilled water before inducing the growth with the addition of gypsum crystals, but in some experiments of $NaSO_4$ and $CaCl_2$ or $Ca(NO_3)_2$ were mixed to obtain higher supersaturation more conveniently [43, 44]. From these studies, it was unequivocally concluded that the

growth rate of gypsum had second-order dependence on the supersaturation. The exception described in [44] is probably the result of secondary nucleation due to higher supersaturation. De Meer *et al.* [45] summarized the previous works well, and compared the results with their own findings using seeds of gypsum found in Nature. Their conclusions were basically congruent with the previously published ones, but in addition they suggested that impurities in the seed tend to result in some deviations during the experiments and lowered the growth rate.

The other, principally different way, how the kinetics of gypsum precipitation can be investigated, is the study of spontaneous precipitation. This way, the nucleation process can be examined too. To perform such experiments, stable supersaturated solutions are needed, therefore the use of the more soluble hemihydrate (see above) turned out to be problematic. Even if it is dissolved quickly, the surface of the crystals makes the heterogeneous nucleation of gypsum possible, hence at high supersaturation, steady state cannot be achieved before the crystallization of the dihydrate [46, 47]. Therefore, supersaturated calcium sulfate solutions were made by mixing solutions of highly soluble calcium and sulfate salts. As expected, supersaturation has the biggest impact on the induction time, which can decrease from hours to as low as seconds at high supersaturation [48-50]. The precipitation seems to be independent of pH providing that sulfate does not undergo protonation and the hydrolysis of calcium is negligible [51]. Experiments carried out at various temperatures made it possible to calculate the activation energy of the nucleation process, and to suggest a surface-diffusion controlled mechanism for gypsum precipitation [52-55]. The results at similar supersaturation can be somewhat different depending on the setup, as many circumstances seems to affect the reaction rate, for example agitation rate and mode, and the material of the reaction vessel [56].

Formation of gypsum is a nuisance in several industrial processes, as mentioned earlier, therefore the kinetics of its precipitation under special conditions were also investigated. Microscopic studies on the nucleation and crystal growth of gypsum on heat-exchanger surfaces showed that gypsum nucleation takes place directly on these surfaces, the roughness and imperfections accelerate the process, and the different faces grow at different rates [57, 58]. The behavior of the reaction was investigated multiple times at higher ionic strength, usually in the presence of different amounts of NaCl, or in some special case studies, in brines [25, 42, 59-62]. This information can be useful in desalination processes along with the experiments of crystallization on membranes [63, 64]. Even some model studies were carried out mimicking the circumstances of boric and phosphoric acid synthesis [65, 66].

Recent studies even suggest a rather complex precipitation pathway for gypsum formation. During the analysis of early stages of the process, amorphous calcium sulfate was found to be formed, which transformed to dihydrate in a stepwise process through the intermediate hemihydrate form [67-69]. The interesting aspects of these reports are that the experiments were carried out around room temperature, where the dihydrate should be the only stable form of calcium sulfate. The formation of hemihydrate nanoparticles suggest that they have much lower solubility than the bulk crystals. These small particles can then aggregate and transform to dihydrate. While it is suggested that gypsum can precipitate through this pathway, the authors state that the direct precipitation of dihydrate can still not be excluded as a possible mechanism.

During the experiments investigating the crystallization of gypsum, numerous experimental methods were used to follow the kinetics of nucleation and crystal growth of gypsum. One of the traditional methods is the sampling of the reaction slurry and determining the calcium content of them by titration with EDTA [35, 37, 38, 59]. Maybe the most popular technique is conductometry, probably because of its simplicity and quick (practically instantaneous) response time for the changes in the solution composition [25, 40, 43, 45, 53,]. It can also be used in coupled set-ups to keep the supersaturation constant and get information from the volume of added calcium and sulphate solutions [41, 44, 52]. Calcium ion selective electrode was used in similar setup to keep the Ca-activity in the solutions constant while measuring the added volume of other solutions [51]. In some cases, the microscopic analysis of the precipitated crystals provided the information needed about the nucleation or the growth of the crystals [48, 57, 58, 64]. Measuring the transmitted and scattered light or turbidity of the reaction slurry is also suitable for the determination of the induction time of the precipitation [25, 54, 59, 60]. However, its use to follow reactions with high initial calcium sulfate concentration can be limited by the vast amount of solid in the system. Examples of measurements based on monitoring the variation of sulfate concentration during the reactions can also be found, which can be of use if other techniques fail to work or need to be verified [56, 62]. Looking into the huge amount of literature available, we can even find some really unusual techniques which were used to monitor the crystallization of gypsum, such as radioactive tracing [42] or quartz crystal microbalance [49, 50].

One can see that the kinetics of gypsum precipitation received a lot of attention, and still receives today. While a large number of factors have already been investigated in this matter,

a kinetic model that can describe the precipitation of gypsum in a wide concentration range is still missing.

2.2.2. The effect of inorganic additives on gypsum crystallization

As we mentioned earlier, the chemical environment in which the precipitation takes place can immensely influence both the nucleation and the crystal growth. Realistically, in every reaction there are impurities present, which makes the investigation of their effects and behavior crucial. The most frequent species present are residual or contaminating foreign ions. Sodium chloride is a typical example. It can influence the nucleation kinetic of gypsum indirectly by changing the solubility of calcium sulfate, and enhances the growth rate, too [59, 60]. As the changes in ionic strength affect the activity of the ions, with the addition of ionic species, such effects are commonly present. Investigating the solubility of gypsum in different metal-sulfate solutions also suggests that in solution, they have similar effects and change the solubility of gypsum almost identically [70]. However, metal ions can affect the reaction through interacting with the precipitating crystals, and significantly modify the kinetics of the reactions.

Over the years, the significance of various metal ions was tested in the precipitation of calcium sulfate. Since magnesium is often present in industrial processes involving gypsum, it is one of the most frequently studied inorganic additives. It was found to be an effective inhibitor in calcium sulfate precipitation under various circumstances increasing the nucleation time and rate of crystal growth [28, 71-77]. Its effect is highly dependent on the concentration of the additive used; with increasing concentration, the inhibiting effect also increases. The magnesium ions are capable of binding on the surface of calcium sulfate, at kinks, on planes or even replacing the calcium in the structure [76], thus interfering with the constant growth of the crystals. Despite this, the incorporation of magnesium to the solid is not necessary [77]. The interaction of magnesium with the calcium sulfate surface causes changes in the morphology of the crystals [73, 75, 77].

Cadmium seems to have effects similar to those obtained for magnesium on the precipitation of calcium sulfate. Several studies were dedicated to the effect of cadmium, with and without further additives [71, 72, 78]. It was found that cadmium also can efficiently inhibit the precipitation by binding on the crystal surfaces. On the other hand, it has very similar properties to calcium-like ionic radius and sulfate complex formation constant, hence it was found to be incorporated in calcium sulfate [79].

Iron is a recurrent impurity in limestone, thus it is often present in processes using lime. Therefore, knowledge of its effect on calcium sulfate precipitation is important from an industrial point of view. Several experiments were carried out in the presence of ferrous- and ferric ions showing that they have some inhibiting effect on the reaction: Fe^{3+} is more efficient than Fe^{2+}, probably due to its higher charge [71-73, 75, 80]. They also modify the morphology in a similar way as the ones mentioned earlier [75, 80].

While these are the most commonly studied ions, many others were looked at in gypsum precipitation reaction like nickel (Ni^{2+}) [81], lead (Pb^{2+}) [71], chromium (Cr^{3+}) [72, 80], copper (Cu^{2+}) [72], potassium (K^{+}) [77], lithium (Li^{+}) [77], and even some lanthanides [82]. They generally affect the reaction in similar ways as magnesium, cadmium and iron, but have varying efficiency in inhibition.

There is, however, an odd metal ion, which in contrast with the ones presented so far does not inhibit the precipitation of gypsum. Aluminum ions were found to decrease the induction period of the reaction, and even can enhance the growth rate of the crystals [28]. This effect must be kept in mind, as it can spoil the effect of organic additives used to prevent or inhibit the precipitation of calcium sulfate [83].

2.2.3. The effect of organic additives on gypsum crystallization

It was shown several times that metal ions were capable of slowing down the precipitation of gypsum; however, complete inhibition is not possible. Organic additives proved to be much more efficient in doing so, therefore various compounds were used to manipulate the crystallization process. Even the first reports, made on studies in this field, talked about possibly inhibiting the crystallization reaction [35, 36]. They found that the most adequate type of additives were the ones capable of binding on the surface of the crystals forming, thus altering the growth process of the crystals. Organic compounds with functional groups capable of forming complexes with calcium ion solution may be able to act in the same (or similar) way on the crystal surface. Up until today, it is understandably a popular and widely investigated topic considering the associated problems found in several industrial processes. Over the years phosphonates and carboxylic polymers yielded the most remarkable results in the field, and many other potentially useful compounds were identified by the researchers.

Phosphonate groups can be strongly bound to calcium ion making them an obvious choice as inhibitors in gypsum precipitation; they are often used in commercially available antiscalants [84]. Several studies prove that they are potent inhibitors, even in small amounts,

they can drastically increase the nucleation time, and if the supersaturation is not too big, complete inhibition is possible [85-90]. Studying the effects of tetraphosphonates, a possible mechanism of surface bonding was proposed by looking into the interatomic distances of the compounds. They suggested that two phosphonate group could bind to a single calcium atom replacing the water molecules or if the structures allow it, different phosphonate groups can bind to neighboring calcium atoms forming chelate-like surface-complexes [89]. Since these additives also affect the crystallization through surface-interactions, it is expected that they can alter the morphology of the precipitating crystals. It was found that at elevated temperature and in acidic media, they are still capable of slowing down the process [91]. Comparing their effectiveness to other organic additives utilized in this reaction, the phosphonates are usually "top-performing" inhibitors [89, 92]. While they are very effective inhibitors, if used in large amounts, phosphonates are considered to be environmentally "unfriendly", therefore if possible, they are avoided in large-scale applications.

One alternative for phosphorous-free additives are polycarboxylates. They were found to be potent inhibitors for gypsum precipitation even in the earliest studies [36], which potency can be enhanced by adjusting the pH of the reaction mixture to the experimentally found optimal value or by building other functional groups (for example hydroxyl and amino groups) into their structure to facilitate surface bonding [93]. The most frequently used polycarboxylates are poly(acrylic acid) and poly(maleic acid), and several others were applied successfully as inhibitors [93-100]. It was found that the size of the polymers can also affect its efficiency; with increasing average molecular weight of poly(acrylic acid) the inhibiting effect decreased systematically [94, 96, 100]. Naturally, because of the surface interaction between these additives and gypsum, they are also capable of modifying the morphology of the crystals. Since gypsum is an undesirable precipitant in various processes, inhibitors need to work under diverse circumstances. Polycarboxylates were tested successfully under close-to-standard circumstances [93, 94], at elevated temperature [95], in acidic media [98], in industrial water models [97] and retarded scaling on heated surfaces [96], proving their usefulness in many aspects. However, just like phosphorous-containing antiscalants, some of these polymers being non-biodegradable, like poly(acrylic acid), represent considerable environmental risk, therefore their use is restricted. In recent years, some "green", biodegradable polymers were tested instead as potential substitutes in water treatment during scale inhibition [99, 100]. The efficiency of these polymers is variable, some of them (*e. g.*, poly(aspartic acid) and poly(epoxysuccinic acid) performed well during the test experiments.

The inhibiting efficacy of the groups of additives mentioned above is outstanding, but they are not the only ones applied. Some macromolecules, such as bovine serum albumin, humic acid and sodium alginate were able to suppress the bulk crystallization of gypsum, but in reverse osmosis experiments they enhanced surface nucleation decreasing the membrane permeability [101]. The addition of surfactants has variable effects. The addition of cetyltrimethylammonium bromide (CTAB), a cationic surfactant seems to decrease the nucleation time and enhance the growth rate, while sodium dodecyl sulfate (SDS), an anionic one has opposite effects, it increased the nucleation time and decreased growth rate [102]. Some amino acids were found to be efficient in delaying the growth of gypsum in seeded experiments with low supersaturation [78]. Since polycarboxylates are very efficient inhibitors in gypsum precipitation, it is logical to assume that small molecular weight di- or tricarboxylic acids may also have this effect. A number of them were tried as additives with varying success, but it is certain that citric acid stands out from them [103-105]. As citric acid is the main additive used in our work, its effects will be discussed in detail in a separate section.

2.2.4. The effect of citric acid on gypsum crystallization

Citric acid became a popular additive in gypsum crystallization for multiple reasons. As mentioned above, its efficiency is much higher than that of other carboxylic acids. It is easier to handle than poly(carboxylic acids), since accurate mass measurement is possible, and its behavior under different circumstances is easier to investigate. Also, it is present in Nature, and is part of natural biological processes, therefore it does not present an environmental threat; it is truly one of the "green" organics. These reasons, and in addition to this, its moderate prize makes citric acid a promising candidate for inhibiting calcium sulfate crystallization during various processes.

Studies on the nucleation kinetics of gypsum in the presence of small amounts of citric acid showed that it could increase the induction time of the reaction. Experiments carried out with slightly varying temperature, additive concentration and moderate supersaturations made it possible to calculate the variations in the interfacial tension between gypsum crystal and the aqueous solution of citric acid [106, 107]. The presence of citric acid is also able to modify the morphology of the crystals forming. The extent of this effect depends on the experimental parameters employed and the concentration of the additive [108-110]. If their individual contributions are determined, the information can be useful for various processes, because with varying morphology and crystal size, the filtering properties of the solid

change. This parameter is critical for example in the wet process of phosphoric acid production [111] and wet flue gas desulfurization process [112]. The effects of citric acid can also be utilized in the construction industry. The retarded settling time of gypsum provides more time for shaping the plaster, but can also decrease its compressive strength [113, 114]; it can prohibit the pre-curing of gypsum during gypsum particle board manufacturing [115]. It is a moderately effective scaling inhibitor in pipes at elevated temperatures [116] as well.

The inhibition effect can be partly explained by the complex formation of citric acid and calcium ions, hence decreasing the supersaturation of the solution. However, this effect is not sufficient to achieve the observed efficiency in the inhibition of the precipitation, as Ca^{2+} and SO_4^{2-} are present in vast excess compared to citrate [104, 110]. As presented earlier, additives containing carboxylic groups are able to interact with the surface of the gypsum crystals, which could be a viable explanation for the inhibiting performance of citric acid. Molecular modelling was used to calculate the distances between the carboxylic groups of citric acid (3.5 Å) and was compared to the shortest Ca^{2+}-Ca^{2+} distance (3.7 Å) of the (1 1 1) crystal face of gypsum, which suggests that the formation of preferential (stable) surface complex comprising two surface metal ions and two carboxylate moieties of the same citrate ion is possible [117, 118]. Similar results were found later implementing the initial findings and claiming that the closest Ca^{2+}-Ca^{2+} distance on the (1 2 0) plane makes it another preferable adsorption face [103, 113]. A recent study using molecular dynamics simulation appeared to prove that the affinity of citrate compared to L-(+)-tartrate for binding on the surface of gypsum is larger, which explains the differences between their inhibiting effects [119]. Considering also that the (1 1 1) plane seems to be the fastest growing face of gypsum in aqueous system [110, 120], it can be said that the outstanding inhibiting performance of citrate ion is a result of its high surface-complex forming affinity on the quickly growing sites of gypsum.

Citric acid is used as additive in many processes where the inhibition of gypsum precipitation or control over the forming crystals is needed. However, there are still some uncovered areas regarding the feasibility of its use under some circumstances. It is mentioned that pH can affect its inhibiting potential [109, 117], but (rather surprisingly) a detailed investigation on this topic is still lacking. It was shown that in some cases, it can be an outstanding inhibitor, but the limits of its effect are still unknown. Is it also effective at high supersaturation? Increasing the additive concentration will always increase the induction period? Also, its efficiency in solutions with high ionic strength needs some

attention, which data could be useful for processes like desalination or heat-exchange using geothermal waters. Since in these media, the regularly used conductometry is ineffective, the search for other applicable measuring method appears to be also of importance.

2.3. Differential precipitation of $Mg(OH)_2$ from gypsum

As mentioned earlier, gypsum precipitates during some neutralization processes, for example in treatment of acidic mine drainages and waste sulfuric acid, which is an environmentally important topic. During these processes, usually lime (as slake or milk of lime) is used to neutralize the fluids. These highly acidic solutions contain large amounts of heavy metal and sulfate ions, which can be removed by the addition of alkaline slurry. By the addition of lime, due to the alkaline pH, heavy metal ions present will be precipitated as hydroxides, along with gypsum [32-34]. At the end of the process a mixed sludge of metal hydroxides and gypsum is obtained making them both useless for further use, and they have to be disposed.

The precipitation of the metal hydroxides can be separated if the neutralization is carried out in two steps using magnesium oxide or hydroxide in the first, instead of lime [121-123]. This way in the first step, the metal hydroxides are only precipitated and a magnesium- and sulfate-rich solution is obtained. Adding lime to this solution will result in the precipitation of magnesium hydroxide and gypsum. The two slurries can be handled separately, and the useful solids can be recovered. The schematic presentation of the process is shown in Figure 4.

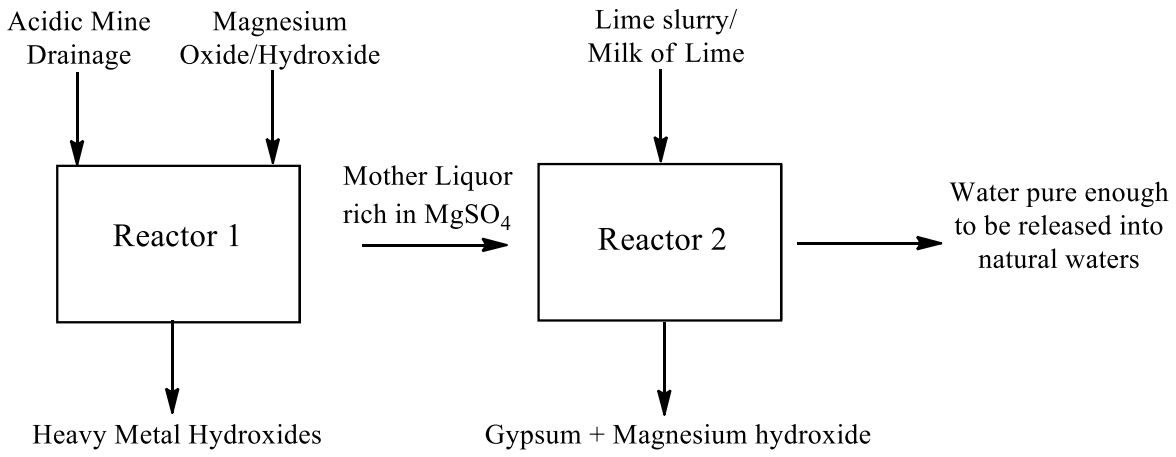

Figure 4. Two-step neutralization of acidic mine drainage using magnesium oxide/hydroxide for separate precipitation of metal hydroxides

To improve the method environmentally and economically even further, in our work, the *in situ* separation of the magnesium hydroxide from gypsum was attempted. The successful separation would allow the use of both precipitants without further treatment; $Mg(OH)_2$ could be recycled in the neutralization treatment, and gypsum could be used in the construction industry.

The method could also be useful in magnesium recovery from seawater, hence improving and facilitating desalination processes. Magnesium can be precipitated in hydroxide form from seawater brines by alkaline solutions; however, it is hard to achieve the desired purity by using lime as hydroxide source [124-126].

To be able to separate the precipitation of magnesium hydroxide and gypsum *in situ* the kinetics of both reactions need to be studied. It was shown earlier that the nucleation and crystal growth of gypsum could be effectively retarded by several additives, therefore here, we will talk about the magnesium hydroxide.

The solubility of $Mg(OH)_2$ (K_{sp} is around 1.38×10^{-11}) is much lower compared to $CaSO_4\cdot2H_2O$ (K_{sp} is around 2.5×10^{-5}) [127, 37], therefore, in stoichiometric reactions its supersaturation will be much higher. Unlike in the case of gypsum, the precipitation kinetics of magnesium hydroxide is naturally highly dependent on the pH of the reaction, since one of the constituents is the hydroxide ion [128]. Of course, the supersaturation is the most important factor making the crystallization of $Mg(OH)_2$ basically instantaneous at high supersaturation [127-131]. Also, while it was shown that the precipitation of gypsum can be slowed by various means, the attempts to do the same with magnesium hydroxide were less successful, sometimes completely futile [127, 130, 132, 133]. All the available information shows that for *in situ* separation of the precipitation of magnesium hydroxide and gypsum, the nucleation of the latter needs to be held back as long as the first solid is separated from the mother liquor.

3. The aims of the work

In the first step of the work, it was aimed to investigate the behavior of gypsum precipitation thoroughly over a wide range of supersaturation. For this, the stoichiometric reaction of

$$Na_2SO_4 + CaCl_2 + 2\ H_2O \rightarrow 2\ NaCl + \underline{CaSO_4 \cdot 2H_2O} \qquad (4)$$

was carried out with systematically varied initial reactant concentration. From now on, these reactions will be mentioned as **single-precipitate reactions** to avoid multiple repetition of reaction equation. The aim of this part of the work was to develop a comprehensive kinetic model, which is capable of describing both the nucleation and crystal growth of gypsum in parallel, and valid for the entire experimentally available concentration range (initial reactant concentration range: 0.04 M – 0.2 M).

To achieve this, robust experimental means are needed. Three methods were employed: *in situ* conductometry, *in situ* direct potentiometry using calcium ion-selective electrode, and *ex situ* inductively coupled plasma optical emission spectrometry (ICP-OES) on withdrawn samples. By comparing the results of these methods, the assessment of the applicability of the various means and their limitations were also intended to be mapped.

As a next step, numerous potential additives were tested in the same reaction as above, and also in a reaction modeling acidic wastewater treatment, that is, gypsum precipitation from the reaction of

$$MgSO_4 + Ca(OH)_2 + 2\ H_2O \rightarrow \underline{Mg(OH)_2} + \underline{CaSO_4 \cdot 2H_2O} \qquad (5)$$

From now on, these reactions will be mentioned as **two-precipitate reactions**.

Since citric acid proved to be the most promising from the additives tested, its effect was scrutinized. Accordingly, the effect of citric acid was studied, firstly, in the single-precipitate system. The pH has little effect on the precipitation of gypsum; however, the protonation of the carboxylic groups of citric acid can lower its inhibiting effect, and it needed to be studied to continue our work. Then the effects of citrate under circumstances highly favoring the precipitation of gypsum (relatively high supersaturation, high agitation speed) were tested. The mechanism and the limits of the retarding effect on the

crystallization were also studied. Since gypsum is often precipitating during the desalination process of seawater, the effects of citrate in seawater-like media was also investigated.

After developing a quantitative picture on the effects of citrate in these reactions, it was used to try and *in situ* separate the precipitation of magnesium hydroxide and gypsum in the two-precipitate system, thus enhancing the economic and environmental viability of the industrial procedures involving similar processes. To optimize the experimental conditions, the effect of the initial reactant concentration, the varying additive concentration and the washing procedure were also investigated. The destination of the additive at the end of the precipitation reaction was also an important issue, since it can affect the quality and usability of the final products, therefore this aspect was also systematically investigated.

4. Materials, methods and experimental procedures

4.1. Materials

Unless otherwise stated, the materials listed here were used without further purification or treatment.

All the chemicals listed in this paragraph were analytical grade products of VWR Hungary: anhydrous sodium sulfate (Na_2SO_4), calcium chloride dihydrate ($CaCl_2 \cdot 2H_2O$), magnesium sulfate heptahydrate ($MgSO_4 \cdot 7H_2O$), trisodium citrate dihydrate ($C_6H_5Na_3O_7 \cdot 2H_2O$), citric acid ($C_6H_8O_7$), sodium dodecyl sulfate ($C_{12}H_{25}NaO_4S$); L(+)-potassium sodium tartrate ($C_4H_4KNaO_6$).

All the chemicals listed in this paragraph were analytical grade products of Sigma-Aldrich (now Merck): sodium hydroxide (NaOH), ethylene glycol ($C_2H_6O_2$), polyethylene glycol ($H(C_2H_4O)_nOH$) average M_n 400, glycerol ($C_3H_8O_3$), sodium D-gluconate monohydrate ($C_8H_9NaO_7 \cdot H_2O$).

The following solutions were the products of Sigma-Aldrich (now Merck): diethylenetriamine penta(methylene phosphonic acid) heptasodium salt ($C_9H_{21}N_3O_{15}P_5Na_7$), 25 w/v% aqueous solution; poly(acrylic acid) sodium salt $(C_3H_3NaO_2)_n$, average $M_w \sim 1200$, 45 w/w% aqueous solution.

Oher materials: calcium oxide in the form of quicklime made from limestone of a natural source (CaO), provided by Lhoist-Minerals lime producer; purified water produced by reverse osmosis.

4.2. Measuring equipment and methods

Variation of the electrical conductivity during the precipitation reactions were monitored using a Jenway 027013 conductivity cell connected to a Jenway 3540 pH and conductivity meter. The built-in sensor of the cell was also used to monitor the temperature.

The pH values of the solutions were measured with a Sentix 62 pH electrode calibrated to 5 points at pH 2, 4, 7, 10, 11.5, using standard buffers.

The potentiometric measurements were carried out with a Metrohm 794 Basic Titrino equipped with a Metrohm combined polymer membrane Ca-ion-selective electrode (Ca-ISE).

To perform ICP-OES measurements, samples were withdrawn from the reaction slurries at given times using a syringe. These samples were quickly (approximately 5-10 seconds) filtered through a syringe filter with 0.45 μm pore diameter. The filtrate was hundredfold diluted in 2% nitric acid to avoid any further precipitation. The measurements were carried out using a Thermo Scientific iCAP 7400 ICP-OES DUO spectrometer.

For the powder X-ray diffractometric measurements, a Rigaku MiniFlex II type Röntgen diffractometer was used. The diffractograms of the precipitates were captured in the $2\theta = 4° – 60°$ range with 2°/min scanning speed, using CuKα ($\lambda = 1.5418$ Å) radiation.

The morphologies of the precipitated solids were studied by scanning electron microscopy using a Hitachi S-4700 scanning electron microscope. This instrument was equipped with a Röntec QX2 spectrometer enabling the elemental mapping of the solids.

UV-Vis spectra of the solutions were measured by an Analytic Jena Specord 210 plus spectrophotometer, using a quartz cuvette.

IR spectra of the solids was measured with two different setups. The spectra in section 5.2.1 were measured using BIO-RAD 18 Digilab Division FTS-65 A/896 FT-IR spectrophotometer using DRS technique. KBr was used for background. For the measurements presented in section 5.3.4., a JASCO FT/IR-4700 spectrophotometer was used which was equipped with a ZnSe ATR accessory and a DTGS detector. With both techniques we studied the spectra in the 4000–650 cm^{-1} wavenumber range with 4 cm^{-1} resolution, accumulating 256 scans.

HPLC measurements of fluid and digested solid samples were carried out with an Agilent 1100 series HPLC using a Grom-Resin ZH type column. The eluent during these measurements was 0.01 M sulfuric acid. The fluid samples were diluted twofold with this solution. To make samples from the precipitated solids, they were added into 0.01 M sulfuric acid in small portions until the newly added crystals could not be dissolved, then the excess solids were filtered and the filtered fluid samples were also diluted twofold with the eluent. These dilutions were necessary to avoid solubility issues during the measurements.

4.3. Experimental procedures

4.3.1. Kinetics of gypsum precipitation

To study the kinetics of the precipitation reaction of $CaSO_4 \cdot 2H_2O$, the stoichiometric reaction of Na_2SO_4 and $CaCl_2$ (single-precipitate reaction, equation (4)) was carried out.

For this, 50 – 50 cm^3 solutions were made, containing stoichiometric amounts of reactants and they were mixed to initiate the reaction. These solutions were made of analytical grade solids with exact mass measurements using an analytical balance. To exclude the inaccuracy caused by the uptake of moisture, the Na_2SO_4 and $CaCl_2$ were kept at 100°C for 12 h. The initial reactant concentration of the reactions was systematically varied in the 0.04 – 0.2 M range. The measurements were carried out in a smooth-surfaced, spherical PTFE vessel, which was thermostated in every reaction at 25°C.

For good repeatability, the strict control of the reaction conditions is needed, therefore every parameter able to influence the kinetics were kept constant (as much as it was possible). The same vessel and stirring equipment was used in every reaction. The agitation was performed with a magnetic stirrer with adjustable agitation rate that was set to 300 rpm, always using the same stirring rod. To minimize the changes in the reactions hydrodynamics, even the electrodes were used in the same positions.

The reactions were monitored *in situ* with conductometric and potentiometric measurements using Ca-ISE for the latter. To check the reliability of these methods, ICP-OES measurements were also carried out measuring the exact calcium content of the mother liquor at given times.

To determine if the wall-effect has an impact on the reaction kinetics, a pre-selected precipitation reaction was carried out in three different vessels (the mentioned smooth-surfaced PTFE, a new, also smooth-surfaced glass beaker and a heavily scratched glass beaker), with similar shape and volume, to maintain similar hydrodynamics in each reaction.

After the reactions reached their equilibrium, the precipitates were separated with vacuum filtration through filtering paper with 0.45 μm pore diameter. Solids precipitated in our scouting experiments showed no sign of contaminants, therefore washing of the samples was not necessary in these systems. The solids were dried at 60°C for 12 h, and their structure was studied by powder XRD measurements. Their morphology was also observed by capturing their SEM images. Meanwhile, the final [Ca^{2+}] value (reached when the conductance of the reaction mixture become constant) and thus, the saturation concentration of the filtrates was determined by titration with EDTA in the presence of murexide indicator. This was necessary for the comparison of the different measuring methods.

The calculations, necessary to develop a comprehensive kinetic model applicable in a wide concentration range, were performed using the ChemMech program package [135]. For practically any kind and arbitrary amount of kinetic experimental data and a supposed

mechanism, ChemMech is able to calculate the best-fitted parameter set for that model. The next features are unique for this program package on the field of chemical kinetics:

- Any chemical parameter (e.g. molar absorption, standard electrode potential, molar conductivity etc.) can be fitted together with the rate constants.
- There is no restriction about the complexity of the ordinary differential equation system belonging to the supposed mechanism.
- Practically unlimited number of experimental curves can be fitted simultaneously. ChemMech is also able to evaluate different kinds of experimental data together. For our evaluation, this feature was indispensable, since we wanted to test the plausible chemical models for all the measured data in a single fitting step.

4.3.2. Effect of citric acid on the kinetics of gypsum precipitation

The effects of citric acid were also tested in the stoichiometric reaction of Na_2SO_4 and $CaCl_2$, which was carried out similarly as during the investigation of the reaction kinetics using the same equipment for the experiments (vessel, agitation, electrodes). The solutions, containing the reactants were prepared as described above, the solids were also handled the same way as above to avoid moisture uptake. To test the limitations of citric acid as an inhibitor, reaction conditions favoring the quick precipitation of gypsum were chosen. The initial reactant concentration was selected to be 0.1 M, the stirring rate 300 rpm (magnetic stirring). The pH of the reactions was adjusted using sodium hydroxide when it was needed. The additive was always dissolved in the sodium sulfate solution. The pH of the reactions was monitored during the individual runs using a calibrated pH electrode, while the kinetics were followed by *in situ* conductometric and in some cases, potentiometric measurements using Ca-ISE for the latter.

To investigate the effect of pH on the crystallization rate, it was systematically varied between 3.15 (the pH of the reaction mixture when citric acid is used as additive) and 10.

According to the results obtained, in the reactions to follow trisodium citrate was used ensuring that the carboxylate groups of the additive are deprotonated during the reactions (pH~6.5). The inhibiting limits of citrate ions were tested by systematically increasing the additive concentration in the reaction mixture until the inhibition effect did not change any more significantly with the increasing additive concentration.

After the equilibrium was reached in the reactions, the precipitates were separated from the mother liquor and both were kept for further analysis. The structure and composition of

the solid samples were investigated by powder XRD. The morphologies of the solids were also studied by capturing their SEM images.

To determine if the additive was incorporated in the precipitating solids, the filtrate and the precipitate were both studied. The fluids were analyzed by UV spectrophotometry and the solids by IR spectroscopy, since both measuring methods are capable of detecting carboxylate groups in the samples.

The effect of citric acid was also investigated in solutions with high ionic strength. In these experiments, the stoichiometric reaction of Na_2SO_4 and $CaCl_2$ was carried out with 0.1 M initial reactant concentration, in the presence of 1 M NaCl background electrolyte (which increased 1.2 M by the end of the reaction, from including the NaCl stemming from the reactants) to mimic conditions in seawater. The agitation rate was 300 rpm, and the concentration of additive (citric acid and trisodium citrate) was 1.5 mM. Since the conductivity of the background electrolyte was very high compared to the effect of the precipitation reaction, instead of conductometry, the reactions were followed by direct potentiometry, using Ca-ISE with two-point calibration (initial and final Ca^{2+} concentration).

At the end of the reactions, the solids were filtered, their composition was determined by powder XRD and the morphology was investigated by capturing SEM images of the solid samples, to compare the effect of the inhibitor in the absence and in the presence of background electrolytes.

4.3.3. Differential precipitation of $Mg(OH)_2$ from $CaSO_4 \cdot 2H_2O$

In situ separation of the precipitation of $Mg(OH)_2$ and $CaSO_4 \cdot 2H_2O$ was attempted during the stoichiometric reaction of $MgSO_4$ and $Ca(OH)_2$ (two-precipitate reaction, equation (5)). Milk of lime (prepared from CaO as quicklime of calcined natural limestone) was used as $Ca(OH)_2$ source. The additives were always dissolved in the initial $MgSO_4$ solution.

Preparation of milk of lime

To prepare milk of lime (MoL) with approximately 20 w/w% solid content, 155 g quicklime was slowly suspended in 845 g purified water. The solids were added to the vigorously stirred fluid, later slurry in a cylindrical glass reactor in small portions, to avoid the quick warming of the mixture. For agitation, a shaft stirrer with a screw propeller PTFE shaft was used at 800 rpm. The slurry was stirred for 2 h after the last portion was added, and then, the insoluble grid was separated using a sieve with 300 μm hole diameter. Later, the actual solid

content was determined by measuring the weight loss of a 100 g sample at 120°C after 12 h. To handle the MoL during the preparations of the reactions more conveniently, it was diluted to *ca.* 5 w/w% solid content, and the exact active $Ca(OH)_2$ content was determined by titration with hydrochloric acid using phenolphthalein indicator.

For the reactions, always fresh sample was prepared – no MoL older than 5 days was used, because due to aggregation, sedimentation and uptake of airborne CO_2, the properties of MoL significantly changed after this time period.

The precipitation reactions were performed in the same cylindrical glass reactor, which was used to prepare the MoL, and the agitation system was also the same. 700 rpm agitation speed was used to assure the quick homogenization of the reaction slurry. First, numerous potential inhibitors were tried in the single-precipitate reaction, and then the promising ones were applied in the two-precipitate reaction. Since citric acid proved to be working well in both reactions, it was used as inhibitor for the differential precipitation of $Mg(OH)_2$ from gypsum. The reaction volume was always 1 L. The $MgSO_4$ and the additive were dissolved in purified water and agitated in the reactor. To initiate the reaction, MoL with 5 w/w% solid content containing stoichiometric amount of $Ca(OH)_2$ was added to the mixture. The volume of the latter determined the volume of purified water in which the other reactants were dissolved. The reactions were followed *in situ* by conductometric measurements, and the temperature and pH of the reaction mixtures was also observed. To back up the results of these methods, ICP-OES measurements were carried out on withdrawn samples of the solution at given reaction times.

To analyze the precipitates, they had to be separated from the mother liquor by vacuum filtration. As the precipitation of $Mg(OH)_2$ is practically instantaneous, a sample was taken after 1-min reaction time. The filtration time was highly dependent on the volume of the withdrawn sample. The solid always contained some gypsum impurities, therefore it was washed, keeping both the precipitate and the washing fluid for further analysis. The first filtered fluid was also kept and agitated further for 2 h, until the remaining gypsum precipitated. This slurry was also filtered, and as earlier, the solid and the fluid was kept for analysis. The schematic presentation of the process is presented in Figure 5.

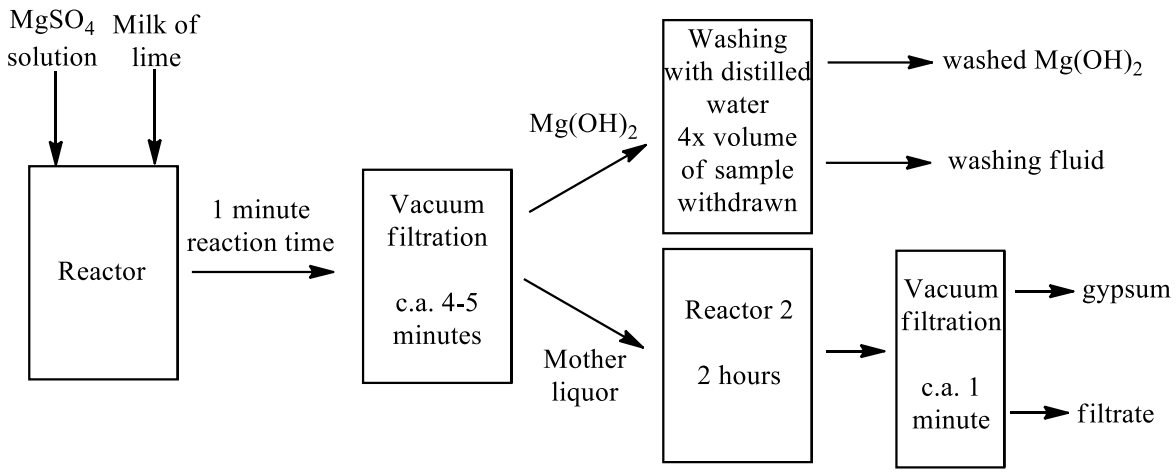

Figure 5. Schematic presentation of the experimental procedure for separating the precipitating solids during the $MgSO_4 + Ca(OH)_2 + 2\ H_2O \rightarrow \underline{Mg(OH)_2} + \underline{CaSO_4 \cdot 2H_2O}$ reaction

The separated solids were analyzed by powder XRD to study their composition. The precipitates were also examined by SEM, and elemental mapping of the samples was also carried out to determine the distribution of the different precipitating solids.

To determine the destination of the added citric acid, various experimental methods were used. Due to the iron contamination of the natural quicklime, the UV spectroscopic measurements of the washing fluid and filtrates were highly unreliable. Therefore, samples of the digested solids, the washing fluid and the final filtrate (after the filtration of gypsum) were measured by HPLC. To further back up the results obtained, the IR spectra of the precipitated solids (obtained both in the presence and in the absence of citric acid) were taken.

5. Results and discussion

5.1. Kinetics of gypsum precipitation over a wide range of concentration

5.1.1. Effect of initial concentration, monitored by different measuring methods

In the first steps of this work, the kinetics of gypsum precipitation was studied in the single-precipitate reactions. The reaction was carried out with systematically varied initial reactant concentration (0.04 M – 0.2 M) encompassing the whole experimentally available concentration range. Going below 0.04 M, the induction time is getting much longer due to approaching the solubility of gypsum which is around 0.015 M in purified water at 25°C [134]. Above 0.2 M initial reactant concentrations, the precipitation is practically instantaneous, thus the time window is too small, and the accurate monitoring of the kinetics of the reaction is practically impossible. The reactions were followed *in situ* with a conductivity cell. The experimentally obtained curves are presented in Figure 6, the observed conductivities were normalized for better comparison of the induction periods.

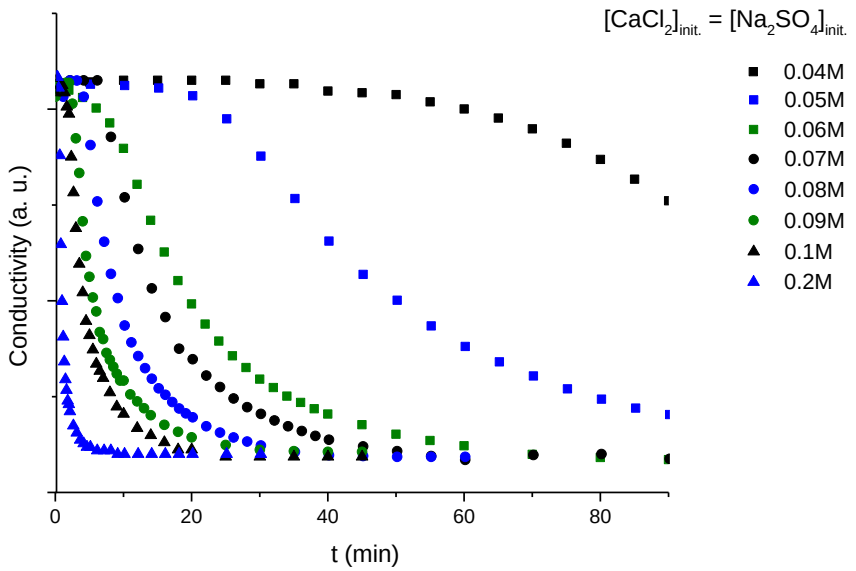

Figure 6. Variation of the conductivity as a function of time during the stoichiometric reaction between $CaCl_2$ and Na_2SO_4 systematically changing the initial reactant concentration in the range of 0.04M – 0.2M. Y axis scale was normalized for better comparison of the induction periods.

As expected, the induction time (in our cases, the time when the measured signal dropped by 0.2 mS/cm, that is, twice the standard error of the conductometric method) is highly dependent on the level of supersaturation. When the concentration is increased, the induction time decreases rapidly changing from approximately 40 min at 0.04 M initial

reactant concentration to a few seconds at 0.2 M. The initial stable phase is followed by the drop of conductivity caused by the depletion of the precipitating ions from the solution. The final conductivity value levels off due to the increasing amount of remaining dissociated NaCl and $CaSO_4$; the latter is determined by the actual solubility at the given ionic strength.

While conductometry can be considered as a robust measuring method under these circumstances, in systems with higher ionic strength, the effect of such reactions could be masked by the background electrolyte. Ca-ISE can be an adequate auxiliary measuring method, since its signal is stable at higher ionic strength like in seawater. However, its response time for the changes in the solution composition is much slower than that of conductometry. To study the limitations and robustness of these two measuring methods, and to determine, under which conditions can one or the other be used, the results obtained by using them were compared to each other and with the results of ICP-OES measurements. For the latter, samples were withdrawn from the reactions at given times, then they were filtered as quickly as physically possible, and diluted in 2 w/w% nitric acid to avoid any further crystallization. These comparisons are shown in Figure 7. The $[Ca^{2+}]$ from the conductivity data was calculated taking the initial and final concentration and assuming linear relationship between the change of concentration and conductivity. The data from the Ca-ISE were processed similarly, also assuming linear change in cell potential with the change in $lg[Ca^{2+}]$.

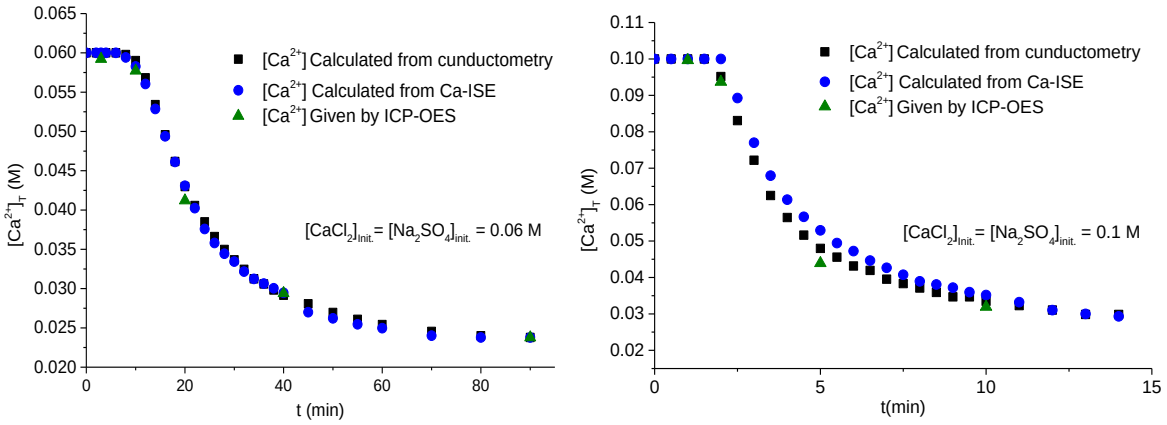

Figure 7. Comparison of the *in situ* conductometric and Ca-ISE methods and the intermittent sampling methods for monitoring the gypsum precipitation in case of an **A:** slower (initial reactant concentration = 0.06 M) and **B:** a faster (initial reactant concentration = 0.1 M) reaction

The results of a slower reaction, with 0.06 M initial reactant concentrations, show that the values from the different measuring methods are basically superimposable, especially considering experimental errors. This suggests that in these "slower" reactions, both *in situ* measurement techniques are fit to follow the kinetics. However, in the "faster" reaction with 0.1 M initial reactant concentration, the Ca-ISE seems to have delayed response compared to the other measuring methods. In the fastest period of the reaction the observed [Ca^{2+}] values gathered with Ca-ISE are more than 10% higher than those from conductometry and ICP-OES.

From these results, we concluded that Ca-ISE is only viable in slower reactions and potentially at higher, constant ionic strength systems. Conductometry seems to be a robust measuring method, able to cover the studied systems at the whole experimentally available concentration range. Therefore, in the following kinetic measurements the data collected from it will be used for further processing.

5.1.2. Characterization of the solids precipitated

After the equilibrium of the reaction was reached, the precipitates were filtered and dried at 60°C. To determine their phase composition, powder XRD measurements were carried out; a typical diffractogram is presented in Figure 8. The Miller indices of the main reflections were marked according to the JCPDS database (# 21-0816).

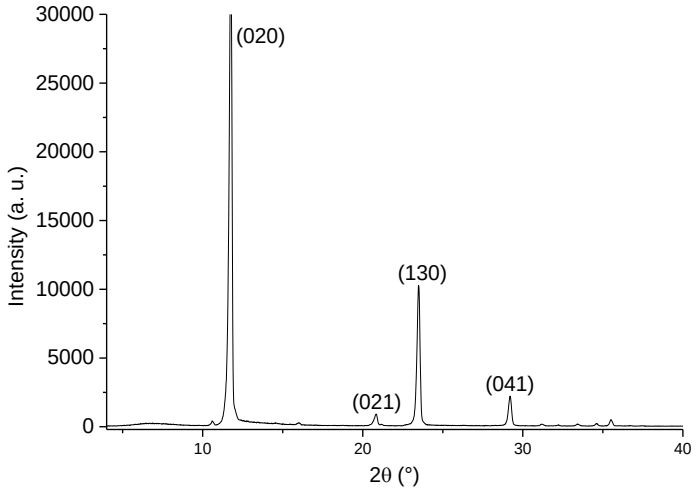

Figure 8. Typical XRD trace of the precipitated and dried solid, $CaSO_4 \cdot 2H_2O$; peaks identified using the JCPDS database (# 21-0816)

The different solids precipitating in reactions with shifting initial concentrations had practically identical XRD patterns. The only solid identified in the precipitates was calcium sulfate dihydrate, neither the hemihydrate nor the anhydrate were present in detectable quantities.

The morphologies of the precipitated solids were also studied, capturing their SEM images. The crystals obtained from different reaction conditions had similar forms and shapes; two examples are shown in Figure 9. Gypsum typically formed rod-like crystals, which was also the case in our reactions; however, the crystals were of variable size, and they were often broken, probably because of the intense stirring applied during the reactions. The difference in the ageing time (due to varying reaction times) can also play a role in this resulting in polydisperse samples.

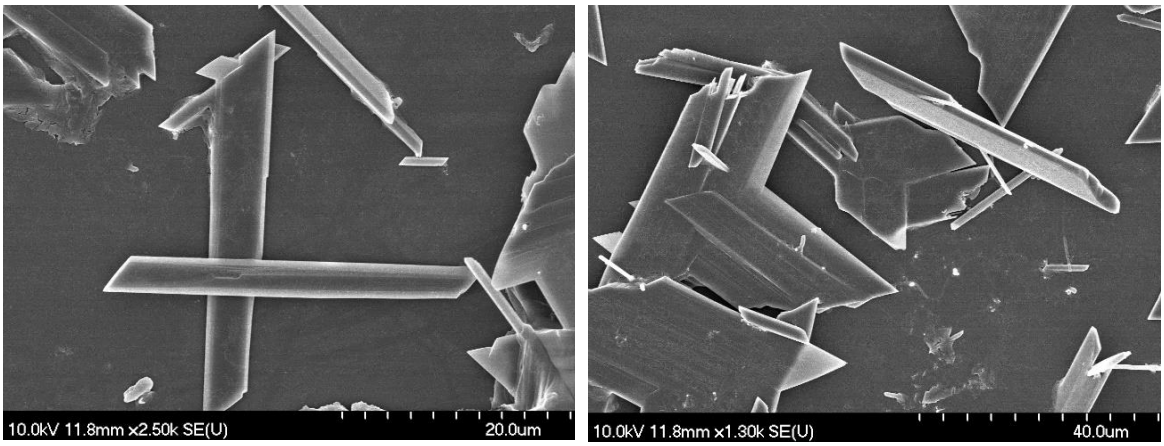

Figure 9. SEM images of the precipitated and dried solid from the reaction of $CaCl_2 + Na_2SO_4 + 2\ H_2O \rightarrow 2\ NaCl + \underline{CaSO_4{\cdot}2H_2O}$ with initial reactant concentrations of **A:** 0.06 M and **B:** 0.1 M

5.1.3. Kinetic model of gypsum precipitation

Processing the results of our measurements, an attempt was made to establish a kinetic model able to describe the nucleation and crystal growth processes simultaneously in the entire studied concentration range. To test our models, the experimentally obtained kinetic curves (Figure 6.) were fitted both individually and simultaneously using the ChemMech program package [135] to calculate the fitted curves.

To start with, the precipitate was assumed to be formed in a simple heterogeneous equilibrium. The wall effect initiating the nucleation was also taken into account. The individual fitting of the curves yielded results that were promising to the naked eye; however, the calculated rate constant values were found to vary four orders of magnitude and

systematically with the increasing initial concentration. This prompted us to improve our initial assumptions and investigate the process further.

First, the influence of the wall effect on the reaction kinetics was investigated. For this, the same precipitation reaction was carried out in three different vessels, under otherwise identical experimental conditions. Besides the previously used smooth-surfaced PTFE vessel a new, smooth-surfaced and a heavily scratched glass beaker, all with similar shape were employed. To be able to precisely measure the reaction rate, reactions with 0.06 M initial reactant concentration were carried out. The reactions were followed by conductometry; the results are presented in Figure 10.

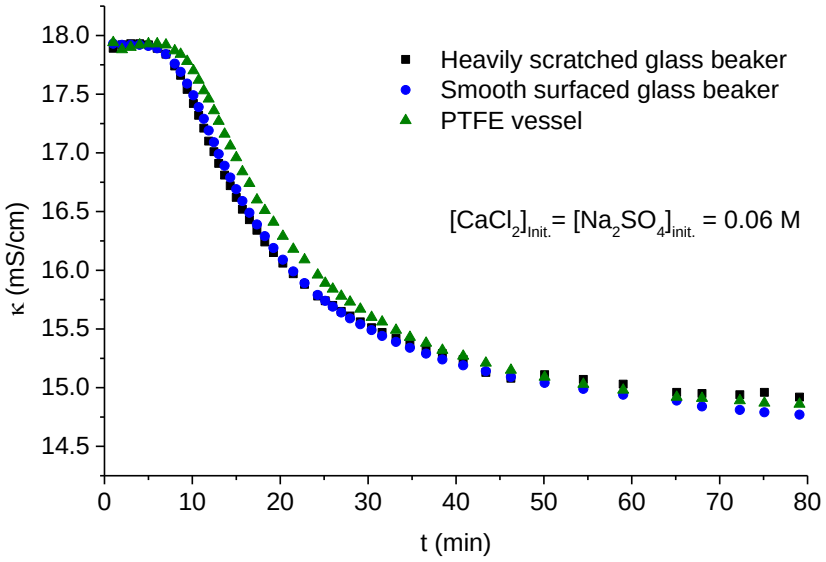

Figure 10. Variation of conductivity during the $CaCl_2 + Na_2SO_4 + 2\ H_2O \rightarrow 2\ NaCl + \underline{CaSO_4 \cdot 2H_2O}$ reaction carried out in different vessels with 0.06 M initial reactant concentration

It can be seen that the curves are superimposable considering experimental uncertainty. This shows that the wall effect can only have minuscule influence on our reactions, and the observed variations of fitted kinetic parameters cannot be caused by adding only the wall effect to the original simple heterogeneous equilibrium model.

To gather more information about our reactions, the measured conductivity data were studied in more detail. The initial and final conductivities in our reactions were compared to the conductivity of undersaturated solutions, as it is shown in Figure 11. The linear fits of the measurement results are also presented.

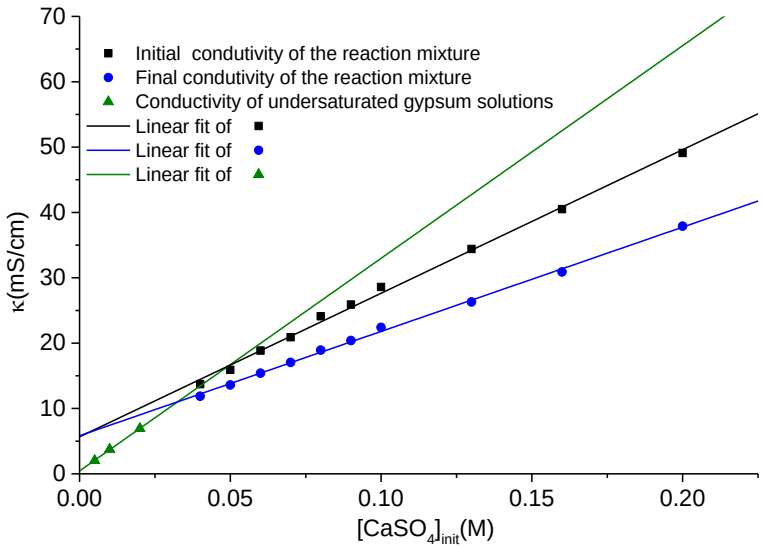

Figure 11. Comparison of the linear fits of the conductivity of unsaturated gypsum solutions, as well as the initial and final conductivities of the measured reaction mixtures

Conductivity supposed to be linearly proportional to the concentration of the ionic species in dilute solutions. However, it can be seen that in our concentration range this is not the case. In explaining the large deviation from this resulting in the non-zero intercept of the conductivity curves relating to supersaturated solutions, two additional effects may be taken into consideration. The formation of the $CaSO_{4(aq)}$ electrically neutral ion-pair can decrease the total conductivity, and the significant ionic-strength dependence of the molar conductivity of the ionic species may also contribute to it.

Considering the above, in our calculations, the variation of the ionic strength was taken into account. Its effect on the equivalent molar conductivity of the present species extrapolated to zero ionic strength was also considered. For the latter, the literature data found on the measured conductivity in aqueous solutions of NaCl, Na_2SO_4, K_2SO_4, KCl and $CaCl_2$ were used [136-142]. These data were fitted with a Davies-like equation [5]:

$$\Lambda_{eq} = a - \frac{b\sqrt{I}}{1 + d\sqrt{I}} - fI \qquad (6)$$

where Λ_{eq} is the molar equivalent conductivity of the pure salt. The calculated values of the constants of this equation for each species are listed in Table 1. The values for calcium sulfate were calculated using the following relationship:

$$\Lambda_{eq}(CaSO_4) = \Lambda_{eq}(CaCl_2) + \Lambda_{eq}(K_2SO_4) - \Lambda_{eq}(KCl) \qquad (7)$$

Table 1. The fitted values of the constants found in the Davies-like equation calculated from the literature data [136-142]. The parameters belonging to $CaSO_4$ were calculated from the others

	a (Scm^2M^{-1})	**b ($Scm^2M^{-1.5}$)**	**d ($M^{-0.5}$)**	**f (Scm^2M^{-2})**
NaCl	126.52±0.20	94.13±0.36	1.772±0.017	6.79±0.11
Na_2SO_4	132.95±0.33	210.5±8.1	2.39±0.19	5.0±1.8
K_2SO_4	154.67±0.08	215.0±2.1	2.211±0.043	1.84±0.33
KCl	150.12±0.04	105.83±0.87	1.962±0.030	5.30±0.07
$CaCl_2$	135.82±0.20	157.7±3.6	2.192±0.089	4.85±0.33
$CaSO_4$	140.35	267.9	2.28	0.42

Considering all the above observations, the following kinetic model was proposed, which was able to properly describe the measured conductivity values handling the nucleation and crystal growth in parallel in the entire investigated concentration range (Equations 8-10).

$$Ca^{2+} + SO_4^{2-} \underset{k_{-1}}{\overset{k_1}{\rightleftharpoons}} CaSO_{4,(s)} \quad \begin{cases} r_1 = k_1 \cdot [Ca^{2+}] \cdot [SO_4^{2-}] \\ r_{-1} = k_{-1} \end{cases} \tag{8}$$

$$Ca^{2+} + SO_4^{2-} \underset{k_{-2}}{\overset{k_2}{\rightleftharpoons}} CaSO_{4,(s)} \quad \begin{cases} r_2 = k_2 \cdot [Ca^{2+}] \cdot [SO_4^{2-}] \cdot \left[CaSO_{4,(s)}\right]^{0,67} \\ r_{-2} = k_{-2} \cdot \left[CaSO_{4,(s)}\right]^{0,67} \end{cases} \tag{9}$$

$$Ca^{2+} + SO_4^{2-} \underset{k_{-3}}{\overset{k_3}{\rightleftharpoons}} CaSO_{4,(aq)} \quad \begin{cases} r_3 = k_3 \cdot [Ca^{2+}] \cdot [SO_4^{2-}] \\ r_{-3} = k_{-3} \cdot \left[CaSO_{4,(aq)}\right] \end{cases} \tag{10}$$

Equation (8) interprets the nucleation process, the formation of new solid particles ($CaSO_{4,(s)}$) constituted from the dissolved ions (Ca^{2+}, SO_4^{2-}) and the reverse reaction, *i.e.*, the dissolution of the crystal embryos. During the simultaneous fittings, the values of k_1 and the initial times should be fitted together; however, doing so resulted in total correlation between these parameters. To avoid this, k_1 or at least one initial time had to be held constant, therefore exact values of these parameters cannot be given, only several set of values for k_1 and the initial times.

The process of crystal growth was described in Equation (9). Since this process can only take place on the crystal surfaces, the virtual $[CaSO_{4,(s)}]$ parameter was incorporated into the equation on the power of 0.67. The calculated value of $k_2 = (7.7 \pm 2.1)\times10^2\ M^{-1.67}s^{-1}$ with the constraint of $\frac{k_2}{k_{-2}} = 3.1\times10^{-5}$, the right side of the constraint being the solubility product

of gypsum at zero ionic strength [143]. This result is independent from the actual value of k_1.

Equation (10) describes the formation and decomposition of the dissolved calcium sulfate ion-pair ($CaSO_{4,(aq)}$). After many calculation runs, it became clear that the reaction was fast and the equilibrium constant was in full correlation with the equivalent conductivity values. When the value of $\frac{k_3}{k_{-3}}$ was fixed, a small modification of the constant values of the Davies-like equation led to similar deviations between the measured and calculated data.

As the presence of the dissolved ion-pair was necessary for proper operation of the model, an attempt was made to describe a new nucleation and crystal growth pathway including this species. The reactions are built similarly as before, they are presented in equations (11) and (12).

$$CaSO_{4,(aq)} \underset{k_{-4}}{\overset{k_4}{\rightleftharpoons}} CaSO_{4,(s)} \quad \begin{cases} r_4 = k_4 \cdot [CaSO_{4,(aq)}] \\ r_{-4} = k_{-4} \cdot [CaSO_{4,(s)}] \end{cases} \tag{11}$$

$$CaSO_{4,(aq)} \underset{k_{-5}}{\overset{k_5}{\rightleftharpoons}} CaSO_{4,(s)} \quad \begin{cases} r_5 = k_5 \cdot [CaSO_{4,(s)}]^{0,67} \cdot [CaSO_{4,(aq)}] \\ r_{-5} = k_{-5} \cdot [CaSO_{4,(s)}]^{0,67} \end{cases} \tag{12}$$

After multiple simulations, it was found that the inclusion of these processes has little to no effect on the results implying that the crystallization steps are going by the individual ions forming new crystals and expanding the growth surfaces.

The measured data and the calculated fittings are shown in Figure 12.

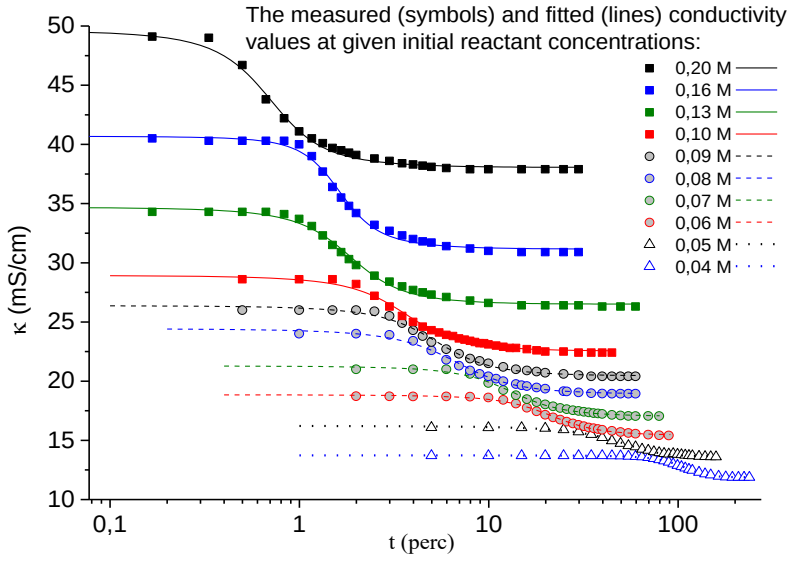

Figure 12. Simultaneous fitting of the measured data with the suggested kinetic model using the ChemMech program package [135], the symbols are representing the measured data, and the lines are representing the calculated data (initial concentration range: 0.04 M – 0.2 M)

The calculated (fitted) data is in very good agreement with the measurement results. The deviation at higher reaction rates can be explained by the hard controllability of the initial part of these reactions. As the induction times are only seconds, even small differences in the actual execution of a given experiment and in hydrodynamics can alter the reaction runs notably. The secondary nucleation is also a factor that can cause these deviations; the SEM images showed that the agitation caused the crystals to brake resulting in new surfaces for growth. Considering all the above, it can be said that the suggested model is capable of describing the precipitation processes simultaneously in the whole experimentally available concentration range.

New scientific results derived from the findings described in section 5.1.:

T1: A comprehensive kinetic model was developed, which is unique in the sense that it is capable of describing the precipitation kinetics of gypsum from aqueous solution in the whole experimentally feasible concentration range. The model is able to include the nucleation and crystal growth processes of gypsum simultaneously.

T2. It was proven for the first time that the formation of the $CaSO_{4(aq)}$ ion-pair had to be taken into consideration for accurately describing the kinetics of the reaction, and that the influence of the wall-effect was negligible under the circumstances applied in this work.

T3. It was proven that under well-defined conditions, Ca-ISE is suitable for accurately measuring $[Ca^{2+}]$ during gypsum crystallization. Ca-ISE was employed by us for the first time to directly measure concentration changes of ions during this precipitation process.

5.2. Effects of citric acid and its limitations as an inhibitor

5.2.1. Scouting experiments; seeking out the most promising inhibitor

To separate the precipitation of $Mg(OH)_2$ from gypsum, the proper inhibitor is necessary to find. Therefore, several additives were tested in the single-precipitate reaction to find potential inhibitors for the target reaction. The initial reactant concentration was 0.2 M and the reaction pH was around 7.

Normally, one of the main determining factors of the reaction rate of the precipitation is induction (nucleation) time, which is not a readily available parameter. In the single-precipitate reactions induction time was defined as the moment, when the level of conductivity dropped by 0.2 mS/cm, which is double the standard error of the measuring method. In the two-precipitate reactions (see later in section 5.3, especially in the fast ones), the presence of other solids, the bigger volume and therefore somewhat slower homogenization can make this parameter unstable (or, in other words, not readily reproducible). Therefore, the use of the half-reaction time was introduced, which is more suitable to quantify and compare the kinetics of the reactions. To obtain this parameter, the measured conductivity data were fitted with the following equation [144]:

$$y = b + \frac{a - b}{1 + \left(\frac{t}{i}\right)^c} \tag{13}$$

where *a* is the initial and *b* is the final conductivity value of the reaction, *t* marks the reaction time, *c* is the slope factor and *i* is the half-reaction time. During the fittings, the initial and final conductivity values were kept constant at the measured values. In the following sections, this method is used for the determination of the half reaction time for more reliable quantification and comparison of the kinetics of the reactions. It is important to note however, that this equation was used only to compare the reaction times, and no further, chemically relevant kinetic data was derived from it.

The potential inhibitors were chosen to contain different functional groups, which were proven to be efficient in the literature slowing down the precipitation of calcium sulfate. Polyols, carboxylic acids, polymers and a phosphonate were added in different concentrations to the reaction. The amounts of the additives used were chosen on the basis of economic considerations; the results are summarized in Table 2.

Table 2. The effect of additives on gypsum precipitation in the reaction of $CaCl_2 + Na_2SO_4 + 2\ H_2O \rightarrow 2\ NaCl + \underline{CaSO_4{\cdot}2H_2O}$ with 0.2 M initial reactant concentration

Additive	Applied concentration (mmol/L)	Half-reaction time (minute)	Standard error of i	Remark
without additive	-	0.75	0.018	
trisodium-citrate(dihydrate)	3.0	**7.61**	0.16	
Na-gluconate	4.0	0.87	0.016	
sucrose	1.5	0.72	0.013	
glycerol	12.0	0.64	0.012	
ethylene glycol	18.0	0.80	0.017	
polyethylene glycol (PEG 400)	1.4	0.68	0.013	
Na-polyacrylate (MW *ca.* 1200)	3.0	-	-	Exceptionally long reaction time
K-Na-tartrate	2.0	0.98	0.014	
SDS	1.0	1.20	0.017	Foaming
diethylenetriamine penta(methylene phosphonic acid) - DTPMP	1.2	-	-	No changes in conductivity for six hours, seemingly colloid formed

Both the high initial reactant concentration, and the relatively small amounts of additives used favor the precipitation reaction. Carrying out the tests it was found that only a handful of these compounds were effective inhibitors even under these circumstances. Besides poly(acrylic acid) and DTPMP, which had remarkable inhibiting results, the mildly effective citric acid was also tested as additive in the two-precipitate reaction. The comparison of these reaction results are shown in Table 3.

Table 3. The effect of promising inhibitors on the reaction of $MgSO_4 + Ca(OH)_2 + 2\ H_2O \rightarrow \underline{Mg(OH)_2} + \underline{CaSO_4{\cdot}2H_2O}$ with 0.2 M initial reactant concentration

Additive	Applied concentration (mmol/L)	Half-reaction time (minute)	Standard error of *i*
without additive	-	1.2	0.007
trisodium citrate(dihydrate)	3.0	3.89	0.020
Na-polyacrylate (MW *ca.* 1200)	3.0	2.50	0.014
diethylenetriamine penta(methylene phosphonic acid) DTPMP	1.2	1.84	0.011

It can be seen that all three additive loses some of its efficiencies, poly(acrylic acid) and DTPMP could not even perform on the level of citric acid, which proved to be the best inhibitor under these circumstances.

Citric acid is known to be an efficient crystallization inhibitor in general, and in gypsum precipitation in particular. It clearly stands out from the other carboxylic acids. Gypsum precipitation inhibition by citrate was studied several times (see section 2.2.4. and references [106-120]) under varying conditions, but its potential in close-to-industrial conditions and at high gypsum supersaturation is still largely unexplored. In our scouting experiments it proved to be the most promising additive to separate the precipitation of $Mg(OH)_2$ and $CaSO_4 \cdot 2H_2O$ (it will be discussed in detail in section 5.3.1.). Since we wanted to apply citric acid/citrate in reactions with near-industrial conditions, its efficiency had to be tested under conditions, where the gypsum precipitation is favored in inhibitor-free systems.

5.2.2. The limitations of citric acid as inhibitor – effect of pH and concentration

While the pH has generally no effect on the solubility and hence on the kinetics of the precipitation of gypsum, it still can influence the effectiveness of the applied inhibitor. As the citric acid interacts with the crystal surfaces by coordinating to the available calcium ions through its carboxylate groups, the protonation and deprotonation of these groups can alter the result of the inhibition. This was mentioned earlier [118], but usually receives little attention in the literature. It was investigated in detail in the single-precipitate reaction with 0.1 M reactant concentration, in the presence of 1.5 mM citric acid adjusting the reaction pH with NaOH. The pH of the systems did not vary significantly during the precipitation reactions; the maximal variation was within 0.1 pH unit. The induction times corresponding to the different solution pH values are presented in Figure 13.

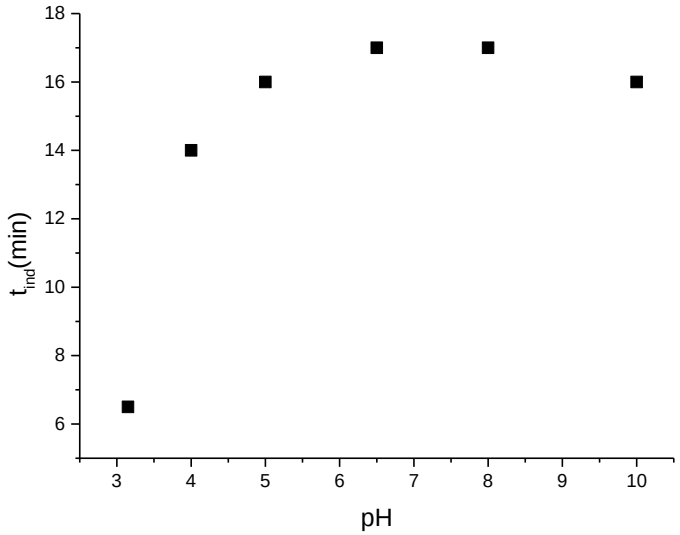

Figure 13. The effect of pH on the inhibiting efficiency of citric acid in the precipitation reaction of gypsum ($CaCl_2 + Na_2SO_4 + 2\ H_2O \rightarrow 2\ NaCl + \underline{CaSO_4 \cdot 2H_2O}$ with 0.1 M initial reactant concentration in the presence of 1.5 mM citric acid)

The pH of the reaction was varied systematically between 3.15 (adding citric acid without further adjustment of pH) and 10. The 6.5 value was achieved by using trisodium citrate without further adjustment of the pH. It can be seen that under pH 5 the reaction is induced faster; the inhibiting efficiency of citric acid is decreasing rapidly especially under pH 4. It is expected, since the protonation of the carboxylic groups of citric acid takes place in this region. Considering only this process should effect the reaction mainly under pH 6, however it is not the case here. The interaction of the additive with calcium ions can affect the process as the metal ions replace the protons by bonding with the ligand forming complexes. The calcium-citrate complexes are dissociated below pH 4 ($logK_{(CaCit-)}$ = 4.85 [145]), which explains the sharp drop of induction time under this pH value. To demonstrate these phenomena, the protonation of citric acid and its complexation in the presence of calcium under our experimental circumstances is shown by two fraction diagram in Figure 14. Above pH 5 the reaction kinetics did not change significantly.

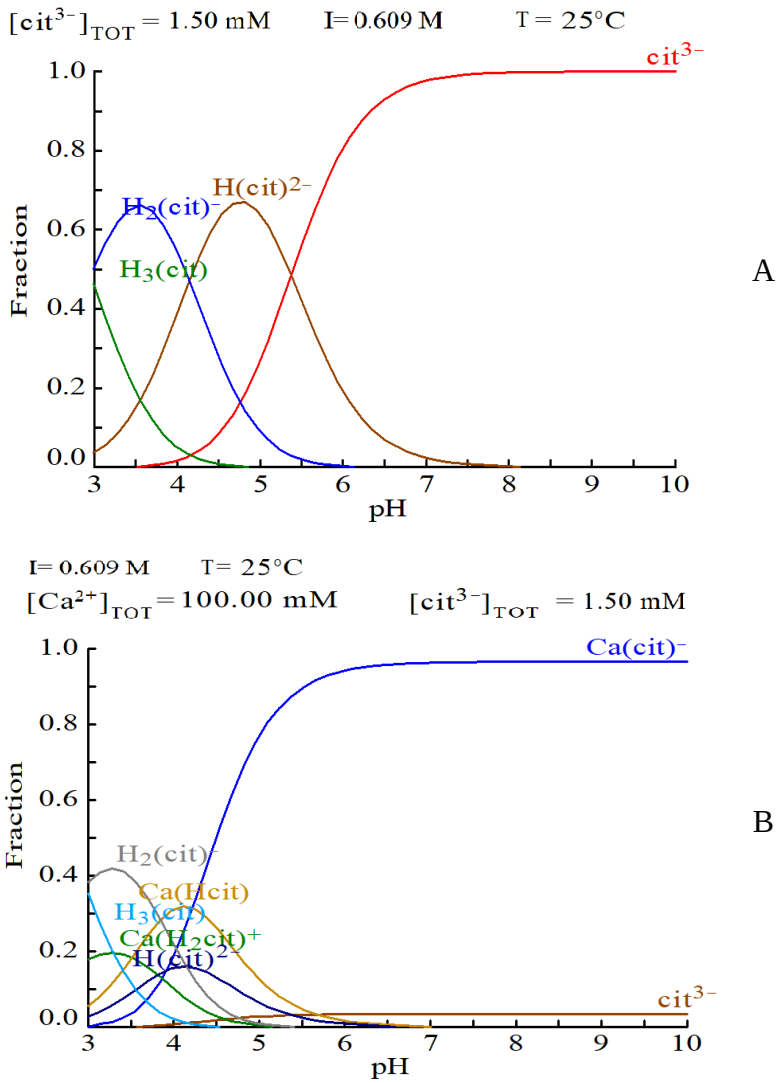

Figure 14. Fraction diagrams of **A:** citric acid protonation in the absence of calcium and **B:** its complexation and protonation in the presence of calcium (circumstances similar to single-precipitate reaction with 0.1 M initial reactant concentration and 1.5 mM citric acid at 25°C) The diagrams were created by Medusa/Hydra software and database

The pH of the reactions is close to neutral when trisodium citrate is used as an inhibitor, therefore in the following reactions this form of the additive was used. The effect of citric acid on the precipitation of gypsum was rarely studied at high supersaturation, therefore not much is known about its potential in these systems. To investigate the limits of citrate inhibition, gypsum was precipitated in the single-precipitate reaction, with 0.1 M initial reactant concentration systematically increasing the concentration of added trisodium-citrate until the inhibiting effect did not increase further with the increased additive amount. The results are shown on Figure 15.

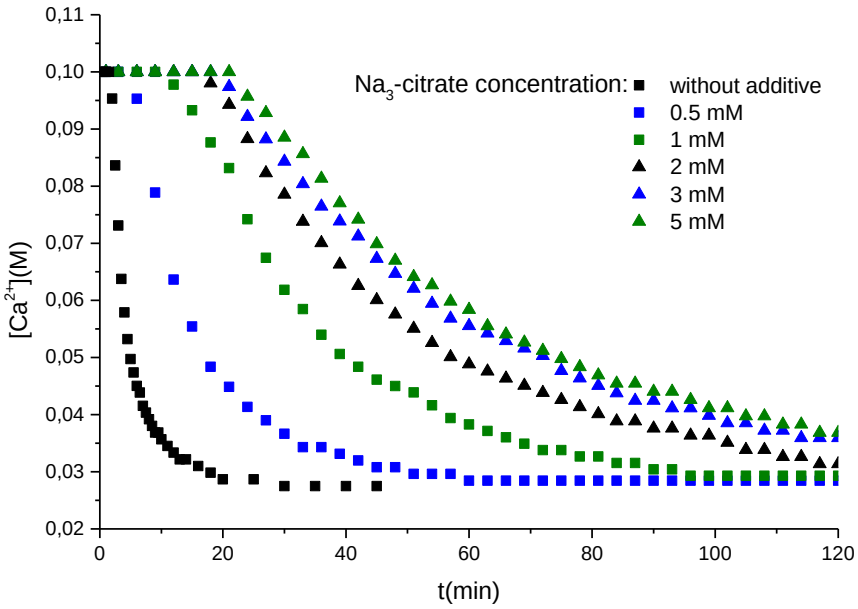

Figure 15. Variation of $[Ca^{2+}]$ (calculated from the results of conductometric measurements) during the stoichiometric reaction of Na_2SO_4 and $CaCl_2$, with 0.1 M reactant concentration systematically varying the concentration of added trisodium citrate

It can be seen that even small amounts of citrate ions increase the induction time significantly, and the effect is increasing systematically with the increasing additive concentration. However, this effect is not linearly proportional to the additive concentration, above 3 mM there are only marginal variations in the induction time and crystal growth process. This can be explained in terms of the mechanism inhibition by citrate: it affects the reaction mainly by interacting with the available Ca^{2+} ions on certain crystal surfaces and when these surfaces become saturated, the inhibiting effect does not increase any further. As the citrate ions are coordinating only to a few crystal surfaces, where the arrangement of the calcium ions are optimal [103, 113, 117, 118], complete inhibition of the reaction is not possible, but the observed relatively long induction times are promising for practical applications.

After the reactions reached their equilibrium, the solids were separated using vacuum filtration, and their composition was determined by powder XRD; the results can be seen in Figure 16.

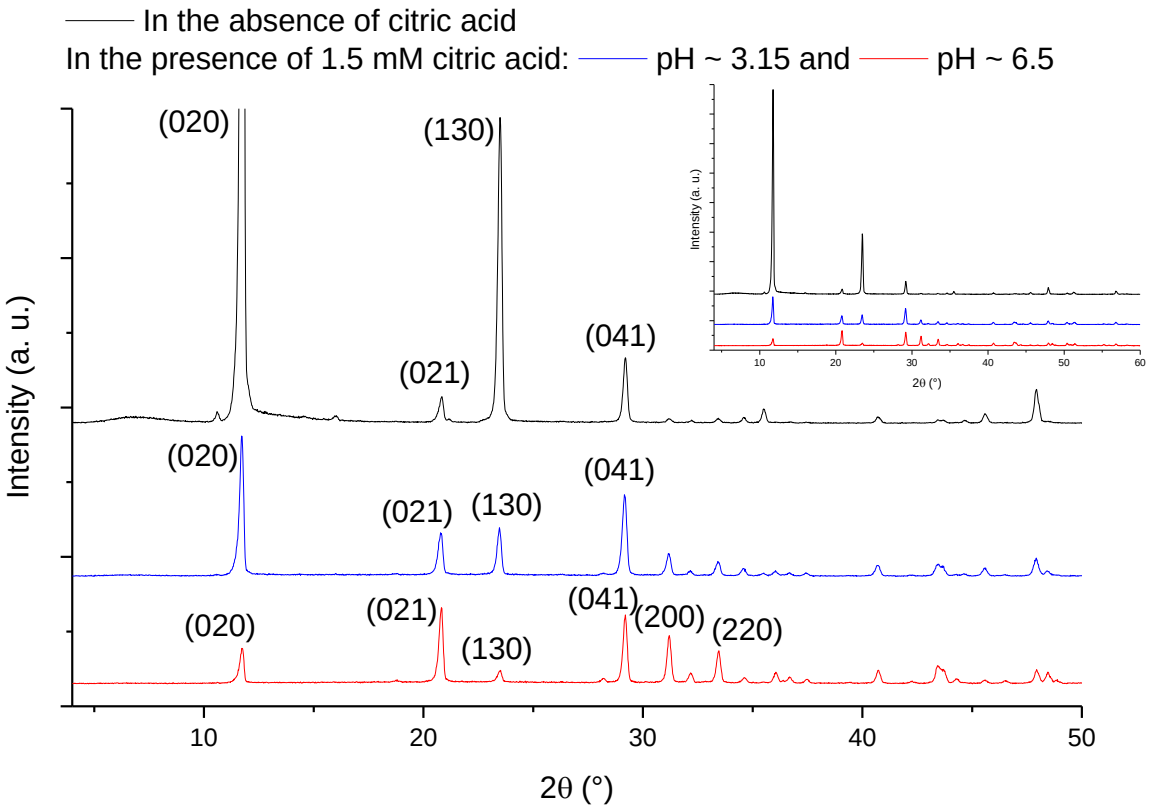

Figure 16. XRD patterns of gypsum crystallized in the absence and in the presence of different forms of citric acid in the stoichiometric reaction of Na_2SO_4 and $CaCl_2$, with 0.1 M reactant concentration (insert presents the same patterns without cutting down the signal corresponding to the (020) reflection of gypsum precipitated in absence of additive); the Miller indices of the main reflections were identified according to the JCPDS database ($CaSO_4 \cdot 2H_2O$: # 21-0816)

It can be seen that the addition of citric acid has major effect on the intensity of some of the reflections and also on the ratio of the individual reflections within one sample decreasing the signal of the most intense peaks to the point where they are comparable or even smaller than the smallest reflections seen in the absence of additive. The observed changes are larger with increased effectiveness of inhibition, which is somewhat expected considering the inhibiting mechanism of citric acid/citrate. The intensities of the reflections corresponding to the crystal lattices with (0 2 0) and (1 3 0) Miller indices significantly decreased when the reaction was carried out in the presence of citric acid (pH ~ 3), and they were even less intense in the presence of trisodium citrate (pH ~ 6.5).

These changes suggest that the morphology of the solid should be changed as well, which is also expected according to the literature [108-110]. The changes were studied by recording the SEM images of the precipitate samples; they are seen in Figure 17.

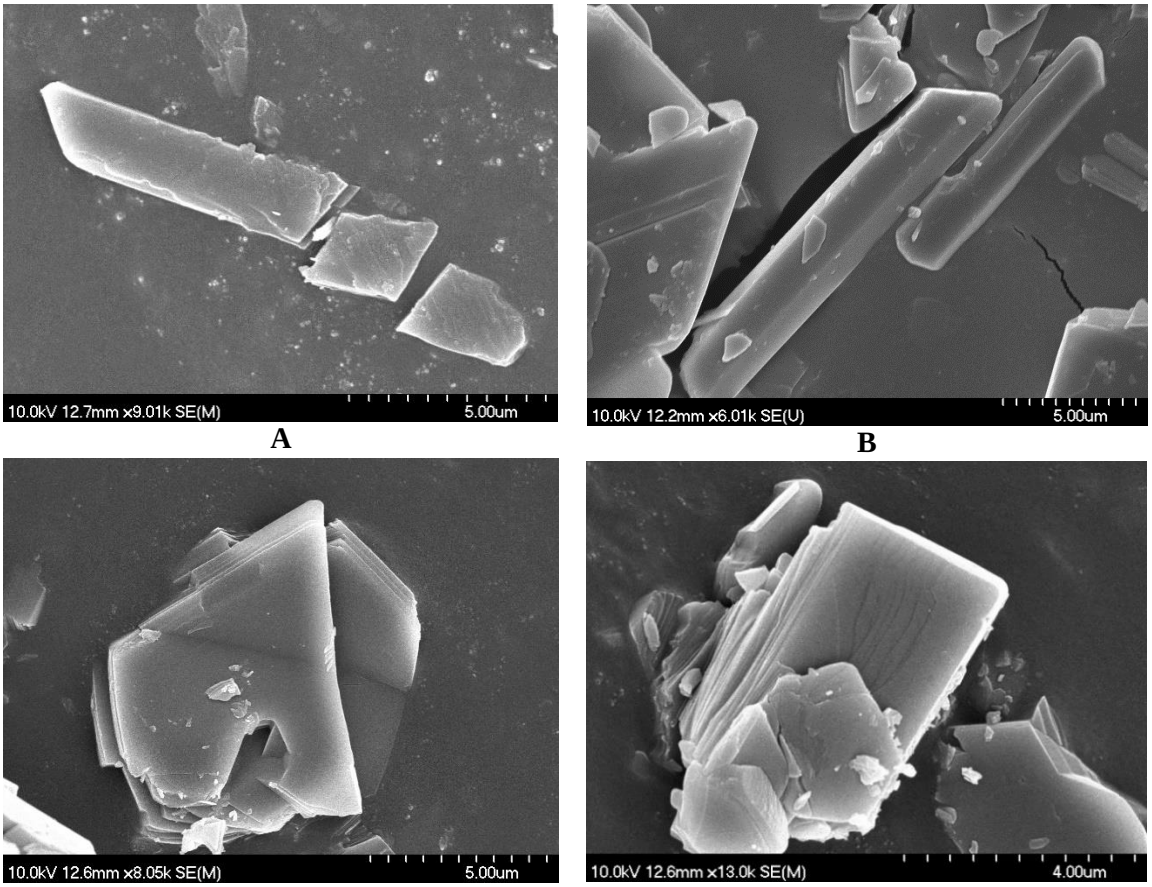

Figure 17. SEM images of the solid samples precipitated in the stoichiometric reaction of Na_2SO_4 and $CaCl_2$ with 0.1 M reactant concentration **A:** in the absence of additive, **B:** in the presence of 1.5 mM citric acid (pH ~ 3) and **C, D:** in the presence of 1.5 mM trisodium citrate (pH ~ 6.5)

One can see that in the absence of additive, gypsum is precipitated in rod-like crystals. Precipitating them in the presence of citric acid, the morphology of the crystals is very similar confirming that the interaction between the additive and the crystals surfaces is not strong enough to cause significant changes. However, as the pH is increased, the crystals tend to form platelets due to the retarded crystal growth rate on specific crystal faces, namely on the (1 1 1) and (1 2 0) crystal faces according to literature [103, 113, 117, 118].

Although the incorporation of the additive in the crystals is unlikely, the quick precipitation of the relatively high amount of crystals could result in the formation of some inclusions. Furthermore, citrate ions could interact with the surface of the crystals, and thus remain on the solids after the reactions. The destination of the additive after the reaction is also an important information for practical applications, since the potential reusability can affect the procedures economic and environmental viability.

To investigate this, first the filtrates of the reaction mixtures were studied by UV spectroscopy. The absorbance of the undiluted samples was too high, therefore those were

diluted fivefold before the measurements. The spectra of filtrates from the reactions with different amounts of citrate present are compared with the filtrate from a blank reaction and with the 0.5 mM solution of trisodium citrate in Figure 18.

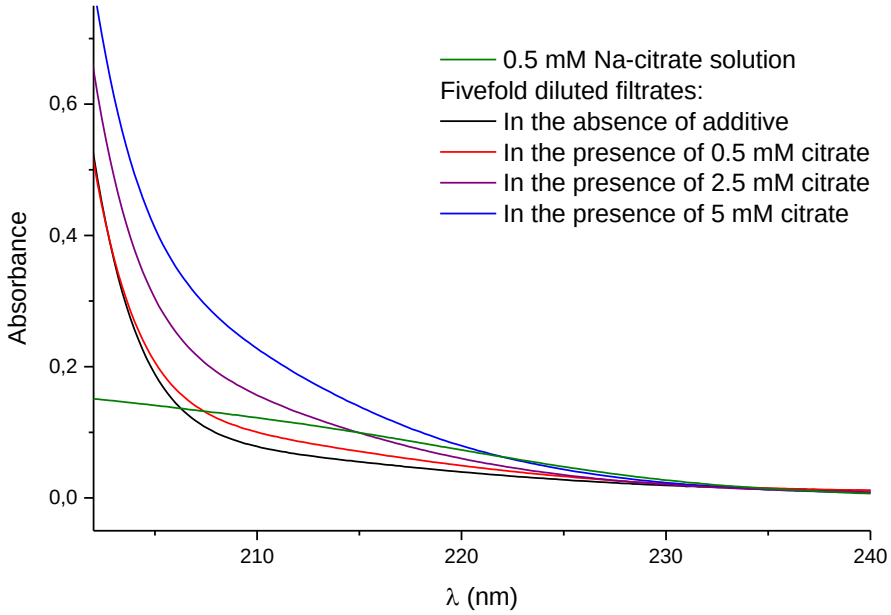

Figure 18. UV spectra of the fivefold diluted filtrates of the precipitation reactions (separated from the solids after the end of the reactions) carried out with systematically varied citrate concentration

It can be seen that in the 200-220 nm region, there are multiple absorbing components. The sharp increase near 200 nm is probably the sign of the remaining sulfate ions in the solutions, but aside from that, systematic increase of absorption can be seen in the 200-220 nm region with the increase of the citrate concentration; probably due to the absorption of the carboxylate groups of citrate. In these samples, the only component with varying concentration is the citrate suggesting that the systematic increase in absorption is caused by the increased additive concentration. The measured absorption increase at 209 nm (typical wavelength for determination of citrate concentration) is linearly proportional to the increase of citrate concentration. This implies that the additive stays in the fluid phase.

To investigate if the solids also contain some of the citrate after the reactions, the IR spectra of gypsum precipitated in the absence and in the presence of 5 mM trisodium citrate were recorded; their comparison is presented in Figure 19.

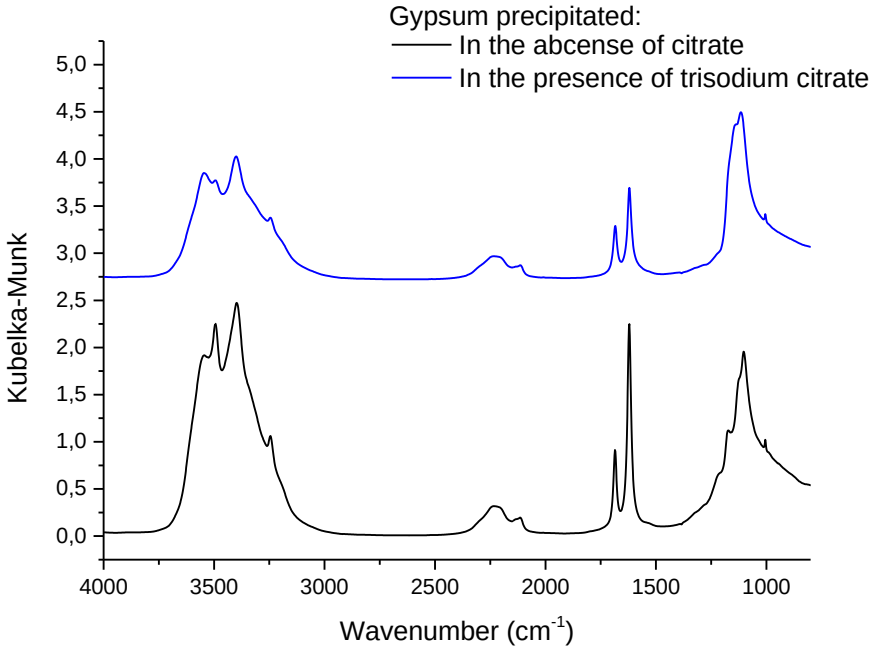

Figure 19. IR spectra of gypsum precipitated in the absence and in the presence of 5 mM trisodium citrate in the stoichiometric reaction of Na_2SO_4 and $CaCl_2$, with 0.1 M reactant concentration

In both spectra, only the characteristic peaks of gypsum can be seen. The signals around 1100-1200 cm^{-1} correspond to the $\nu_3(SO_4)$, the wider bands at 2200 cm^{-1} are combinations of the ν_1 and ν_2 modes of sulfate. The peaks at 1620 and 1680 cm^{-1} correspond to the ν_2 vibrations of crystalline water, the sharp peak standing out of the broad band at the region of 3000-3600 cm^{-1} is the sign of the stretching mode of water [146]. There are no traces typical of organic compounds or the sign of carboxylic groups present suggesting that the precipitates do not contain detectable amount of citrate. These results and the fact that the absorption of the filtrates at 209 nm increases proportionally with the increase of citrate concentration suggest that practically all of the additive stays in the fluid phase.

5.2.3. Effects of citric acid at higher ionic strength, modelling seawater

During industrial processes, numerous circumstances had to be considered, which can alter the result of experiments, and can also change the behavior of the unwanted side-reaction such as gypsum precipitation. Ionic strength is one of these factors, and it is really important in processes involving seawater like the desalination processes. Therefore, the inhibition of gypsum precipitation under these circumstances is an important issue, which had to be studied.

To investigate the effect of increased ionic strength – modeling seawater – on the efficiency of citrate inhibition, the gypsum was precipitated in the presence of 1 M NaCl. Single-precipitate reactions were carried out with 0.1 M initial reactant concentration in the absence and in the presence of 1.5 mM citric acid and trisodium citrate. Since the conductivity of the background electrolyte could mask some of the effect of the precipitation reaction, Ca-ISE was used to follow the reactions. The variation of [Ca^{2+}] calculated from the results of these measurements are presented in Figure 20.

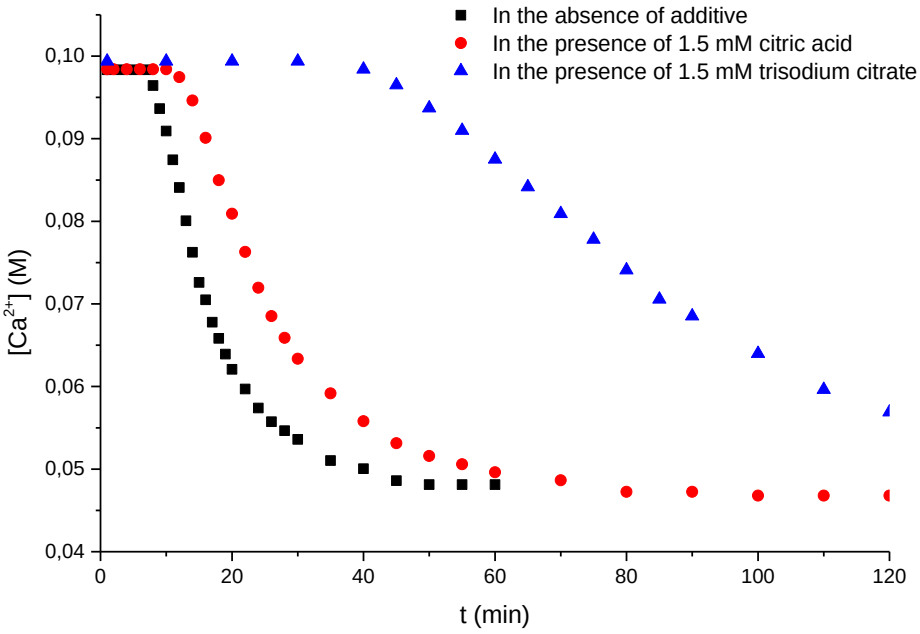

Figure 20. Variation of [Ca^{2+}] (calculated from the results of Ca-ISE measurements) during the stoichiometric reaction of Na_2SO_4 and $CaCl_2$, with 0.1 M reactant concentration and in the presence of 1.0 M NaCl

Looking into the results, it is seen that the reaction itself is slower than without additional NaCl. This is beneficial for the measuring method having a bit slower response time. The phenomenon is probably caused by the higher solubility of gypsum, and thus smaller supersaturation, caused by the higher ionic strength. The concentration of calcium at the end of the reactions also confirms this, and it is in agreement with the literature data available on the effect of NaCl on gypsum solubility [147, 148]. The difference in the inhibiting effect between citric acid and sodium citrate is still similar. This was expected, since the additive is the pH determining factor in these systems. The increased solubility of gypsum also affects the inhibited reactions, in the presence of 1.5 mM citrate, the observed induction period was around 40 min, which is the approximately twice as long as the one

observed in the absence of additional NaCl. These results are very promising for the practical application of citric acid as crystallization inhibitor in high ionic strength environments.

The precipitated solids were studied similarly as before, after the reactions reached their final point, the precipitants were separated from the mother liquor via vacuum filtration. After drying, their composition was analyzed by powder XRD, the captured diffractograms are shown on Figure 21.

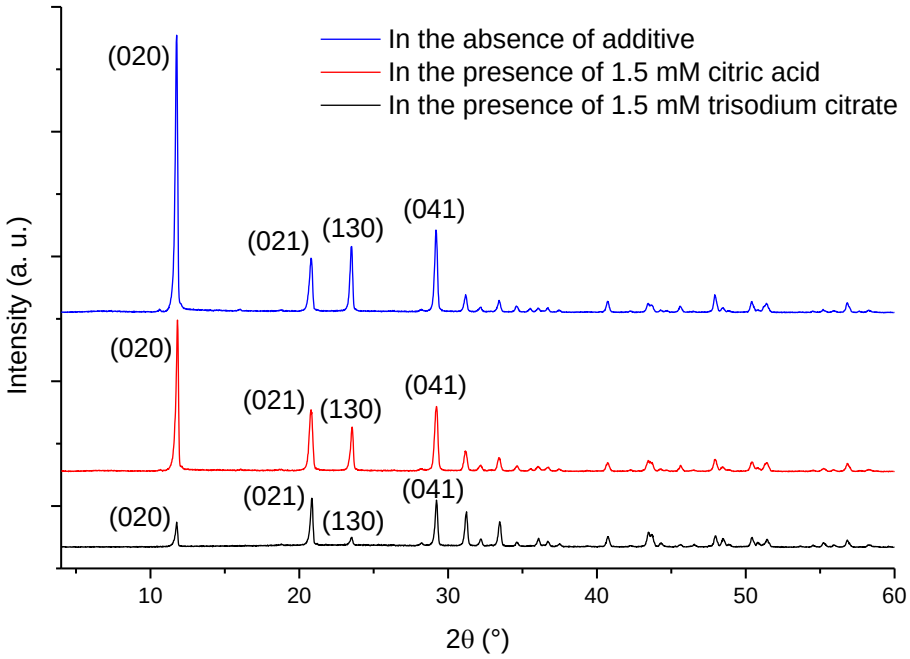

Figure 21. XRD patterns of the solids precipitated during the stoichiometric reaction of Na_2SO_4 and $CaCl_2$, with 0.1 M reactant concentration in the presence of 1.0 M additional NaCl, in the absence and in the presence of different forms of citric acid; main reflections were identified according to the JCPDS database ($CaSO_4 \cdot 2H_2O$: # 21-0816)

The XRD patterns seen in Figure 21 are rather similar to those shown earlier (Figure 16), but the differences between the individual diffractograms are much less pronounced. The reflection of the crystal lattices with (0 2 0) and (1 3 0) Miller indices are not standing out as much as in the small ionic strength system in the absence of the additive. The intensity of these peaks systematically decreases (both absolutely and compared to the other reflections) with the increasing effectiveness of the inhibition.

As we have seen earlier, the solids underwent significant morphological changes in the presence of the inhibitor. In these systems, similar tendencies were observed, therefore SEM images of the solids were captured to study the morphologies of the samples. They are presented in Figure 22.

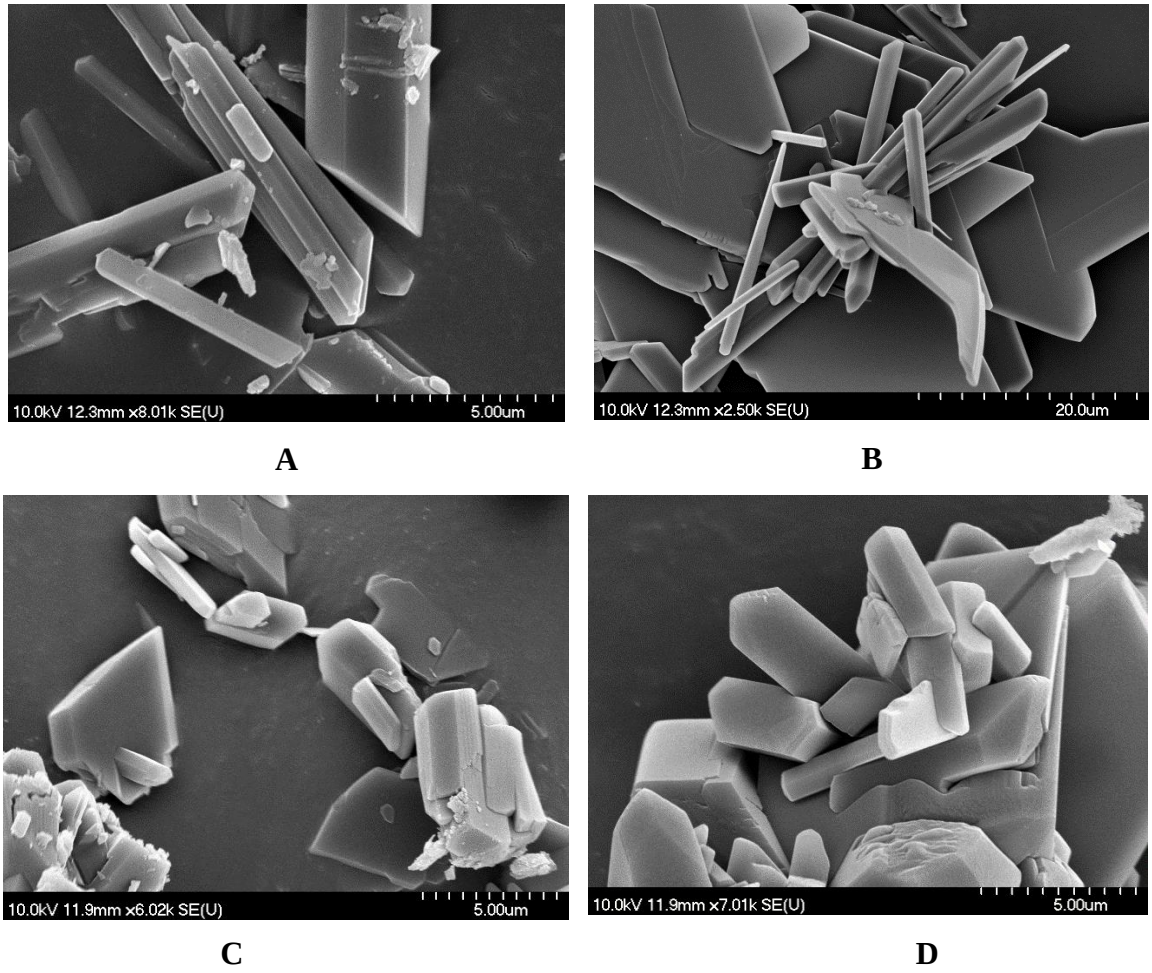

Figure 22. SEM images of gypsum precipitated during the stoichiometric reaction of Na_2SO_4 and $CaCl_2$, with 0.1 M reactant concentration in the presence of 1 M additional NaCl, **A**: in the absence of additive, **B:** in the presence of 1.5 mM citric acid and **C, D:** in the presence of 1.5 mM trisodium citrate

The crystal sizes in every sample seem to be polydisperse, probably due to the breaking of the crystals caused by the intense agitation. The solids precipitated in the absence of additive mainly contain crystals with rod- or needle-like morphology. In the samples obtained in the presence of citric acid some differences can be spotted, but it is hard to differentiate them from the broken crystals, their main morphology is generally the same as of the crystals from the additive-free reactions, they form rods and needles. Looking at the images of the solids coming from the citrate-inhibited reactions, the changes are upfront. Unlike in the systems without background electrolyte, the crystals are mostly forming shortened rods, but plate forms can also be observed in the samples, similar to the ones precipitated in absence of background electrolyte.

Considering the results of our measurements, it can be said that citric acid (in citrate form) can act successfully as an inhibitor of gypsum precipitation even under near-industrial circumstances. Looking into our experiments and the literature we can assume that the citrate ions are inhibiting the reactions through interacting with the surface of gypsum crystals. The structure of the citric acid molecules makes it possible to coordinate to the available calcium ions on different surfaces of gypsum [103, 113, 117, 118]. Akyol et. al. [89] showed how tetraphosphonates are able to coordinate by substituting the coordinated water molecules of the available calcium ions, which is also possible for the citrate ions to do in a similar way. The distance between the carboxylic groups even allows the additive to coordinate to neighboring calcium-ions. It seems like this mechanism would only explain the inhibition of the crystal growth process. However, before nucleation could occur, miniscule particles (smaller than the critical radius, the minimal nuclei size) need to be formed. If the additive can bind to these particles, it could retard their growth which can significantly elongate the induction period [149]. The results of our XRD measurements and SEM images back up that citrate interacts with the surfaces of gypsum. Also the experiments investigating the reaction with varying additive concentration suggest that these surfaces can be saturated, maximizing the inhibiting effect. Increasing the NaCl content of the systems slowed down the reaction, and it seems that the inhibition mechanism is somehow different in the presence of higher amount of chloride ions which probably can slightly alter the process. The higher ionic strength of the processes involving seawater is even beneficial for its practical application, since the solubility of gypsum is higher in these systems and thus the efficiency of the inhibition is higher.

New scientific results derived from the findings described in section 5.2.:

T4. The inhibiting effects of citric acid on the precipitation of gypsum from highly supersaturated solutions were described at various pH values, and the optimum conditions for maximum inhibition efficiency were established.

T5. The effects of citric acid on the precipitation of gypsum in systems without added background electrolyte were compared with high-ionic strength systems mimicking sea water. It was established that NaCl increased the inhibiting effect of citrate, but the morphological changes of the precipitating solids were less dramatic in the presence than in the absence of added electrolyte. This implies that chloride ions change the inhibition mechanism of citrate.

5.3. Differential precipitation of magnesium hydroxide from gypsum

In the third part of our work, an attempt was made to separate the precipitation of $Mg(OH)_2$ and $CaSO_4$ in time during the two-precipitate reaction using additives to slow down the precipitation of gypsum until the $Mg(OH)_2$ could be separated from the mother liquor. During these reactions, milk of lime prepared from quicklime made of natural limestone was used as $Ca(OH)_2$ source.

As it was shown in section 5.2.1, the scouting experiments suggested that the best suited inhibitor to separate the crystallization reactions in the two-precipitate system is citric acid (citrate). It is easier to handle than the other tested candidates (polyacrylate and DTPMP) and most importantly it presents significantly smaller environmental threat than those. Therefore, in the following steps, the optimization of the reaction parameters was attempted using citric acid as an inhibitor of gypsum precipitation to separate the two precipitation reactions.

5.3.1. Effects of citric acid on the reaction kinetics

Since the timeframe before the induction of gypsum precipitation seemed to be too narrow with 0.2 M initial reactant concentration, to efficiently separate the $Mg(OH)_2$, the reaction was carried out with halved concentrations. The temperature of the reaction mixture was recorded in every experiment. During the individual reactions, it did not change more than ±0.5°C. The pH of the system was also monitored, the initial $MgSO_4$ solution was neutral, which changed to around pH ~ 3 upon the addition of citric acid. The addition of the MoL raised the pH to 11.1-11.2, which is in good agreement with the nucleation pH of magnesium hydroxide [128]. This also means that the reaction mitigates any changes in the pH. The variation of the conductivity during the reactions in the absence and in the presence of additive can be seen in Figure 23.

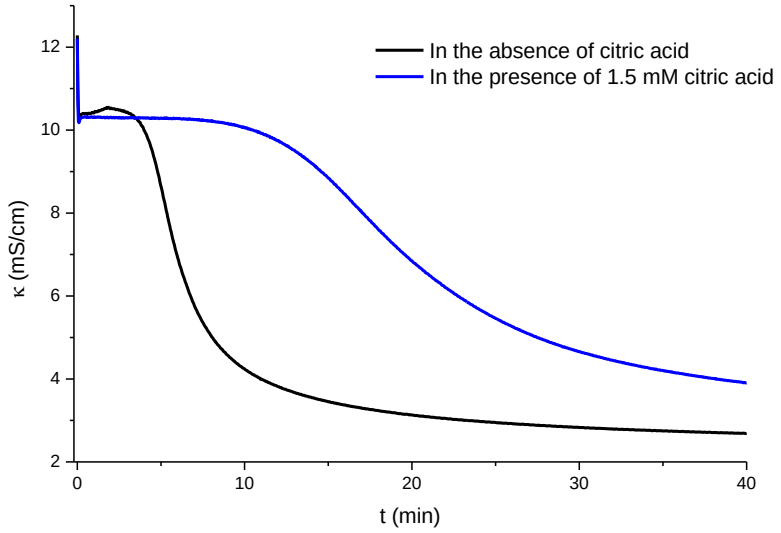

Figure 23. The variation of conductivity during the reaction of $MgSO_4 + Ca(OH)_2 + 2\ H_2O \rightarrow \underline{Mg(OH)_2} + \underline{CaSO_4 \cdot 2H_2O}$ with 0.1 M initial reactant concentration in the absence and in the presence of 1.5 mM citric acid (T = 20°C, in purified water without supporting electrolytes)

When the reaction was commenced by adding the MoL to the magnesium sulfate solution, a drop in solution conductivity can be observed. This is probably the sign of two parallel reactions, the instantaneous precipitation of $Mg(OH)_2$ and the quick dissolution of $Ca(OH)_2$. After this, a short plateau – the induction period – is followed by the slow decline of the conductivity, caused by the precipitation of gypsum. It can be seen that the addition of citric acid increases the duration of the induction period significantly.

To confirm our interpretation of the results of conductivity, samples were withdrawn from an inhibited reaction at given times. The samples were quickly filtered, and the filtrates were prepared for ICP-OES measurements, to determine the variation of $[Mg^{2+}]$ and $[Ca^{2+}]$ during the reaction. The initial ionic concentrations were calculated from the weight of the added salts. The results were then compared with the conductivity data collected, this can be seen on Figure 24.

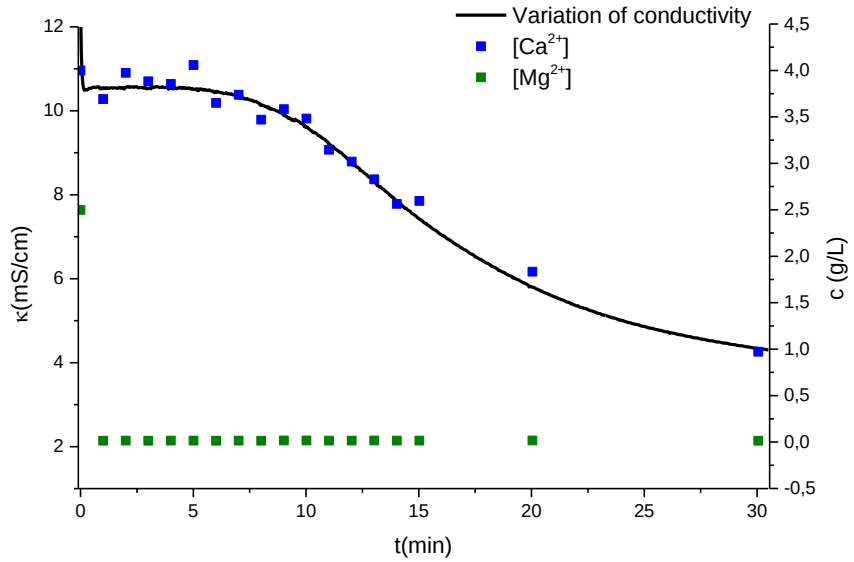

Figure 24. Comparison of the measured conductivity data (left Y axis) and the variation of $[Ca^{2+}]$ and $[Mg^{2+}]$ (right Y axis) according to ICP-OES measurements during the reaction of $MgSO_4 + Ca(OH)_2 + 2\ H_2O \rightarrow \underline{Mg(OH)_2} + \underline{CaSO_4 \cdot 2H_2O}$ with 0.1 M initial reactant concentration in the presence of 1.5 mM citric acid (T = 20°C, in purified water without supporting electrolytes)

The results show that the concentration of magnesium ions indeed dropped instantaneously (by the ICP-OES results, $[Mg^{2+}]$ is in the range of 0.3 – 0.6 % of initial concentration) due to the quick precipitation of $Mg(OH)_2$. The precipitation of calcium sulfate is significantly slower. It can also be seen that the decline of the conductivity is superimposable with the variation of $[Ca^{2+}]$ obtained from the ICP-OES measurements. This suggests that the conductivity can be used confidently to *in situ* monitor the precipitation of gypsum in these reactions.

The 0.1 M initial reactant concentration highly favors the precipitation of gypsum; however, in industrial systems there are several cases, when the reactants are present in concentrations which are much higher than this. Therefore, in a set of experiments, the initial reactant concentration was raised systematically, while keeping the reactant-to-additive molar ratio constant. The results of the conductivity measurements are presented in Figure 25.

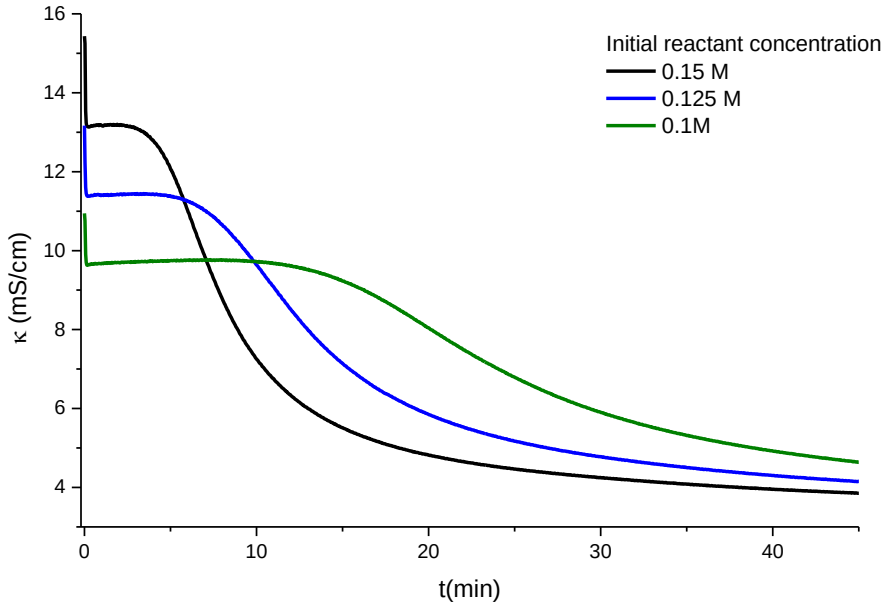

Figure 25. The effect of increasing initial reactant concentration on the variation of conductivity during the $MgSO_4 + Ca(OH)_2 + 2\ H_2O \rightarrow \underline{Mg(OH)_2} + \underline{CaSO_4 \cdot 2H_2O}$ reaction, while keeping the reactant-to-additive ratio constant (the molar ratio of Ca:Mg:citric acid = 0.1:0.1:0.0015) (T = 20°C, in purified water without supporting electrolytes)

It can be seen that the proportional increase of the additive concentration with the increase of the initial reactant concentration was not sufficient, the rate of gypsum precipitation still increased significantly. The half-reaction time at 0.1 M initial reactant concentration was found to be about 23 min, which decreased to just 8.5 min at 0.15 M. These results are not surprising, since the high agitation speed, the increasing supersaturation and the higher amount of solids, and thus potential precipitating sites present are all accelerating factors in the precipitation of gypsum. This has to be considered when planning practical uses. In the second step of acidic mine drainage treatments, the concentration of $MgSO_4$ coming from the first step can vary in concentration, therefore this phenomenon need to be dealt with.

A potential solution could be dilution or the increase of the additive concentration used. Considering the economic viability, the latter is favorable, because it does not increase the amount of water to be treated. To investigate the effect of changing amounts of citric acid used, the reaction with 0.1 M was carried out with different amounts of additive. The results of the conductivity measurements of these reactions are shown in Figure 26.

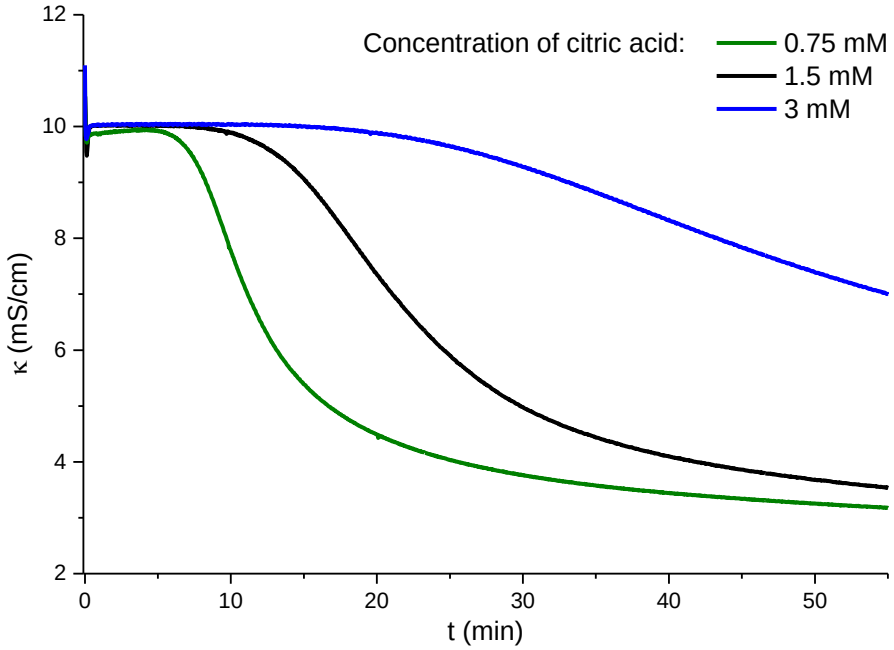

Figure 26. The variation of conductivity during the reactions of $MgSO_4 + Ca(OH)_2 + 2\ H_2O \rightarrow \underline{Mg(OH)_2} + \underline{CaSO_4 \cdot 2H_2O}$ with 0.1 M initial reactant concentration in the presence of different amounts of citric acid (T = 20°C, in purified water without supporting electrolytes)

Changing the amount of the additive had major effect on the reaction rate of gypsum precipitation. Doubling the concentration used earlier (1.5 mM) almost doubled the half-reaction time; from 23 min it increased up to 56 min in the presence of 3 mM citric acid. This effect could be used to compensate the effect of increasing initial reactant concentration. Citric acid is a "green" additive, present in nature, but it still cannot be left in the final fluid in vast amounts, and increasing the additive amount can lower the cost-efficiency of the process. To solve these challenges, it is necessary to determine the destination of citrate after the reaction and its potency to be reused had to be investigated. This will be discussed in section 5.3.4.

As mentioned earlier, the temperature of the reactions was monitored. It was observed that the induction of the reaction by the addition of MoL did not lead to significant temperature change, probably because the heat effects of the different processes canceled each other out. The temperature of the reactions did not change more than ± 0.5°C during the individual runs. The reaction temperature was set by the actual room temperature. After several repeated experiments, it became clear that the temperature has a significant effect on the rate of precipitation. The magnitude of the changes qualitatively corresponds to the Arrhenius law. The relation of the reaction rate and temperature is collected in Table 4.

Table 4. The correlation between the reaction temperature and gypsum precipitation rate during the reaction of $MgSO_4 + Ca(OH)_2 + 2\ H_2O \rightarrow \underline{Mg(OH)_2} + \underline{CaSO_4 \cdot 2H_2O}$ with 0.1 M initial reactant concentration in the presence of 1.5 mM citric acid

Temperature (°C)	Estimated induction time (min)	Half-reaction time (min)
20	10.3	22.8
22	9.1	21.1
24	6.8	17.5
26	5.8	15.7

It can be seen that even small changes in the temperature has significant effect on the precipitation rate of gypsum speeding up the reaction with increasing temperature. Beside the direct effect on the reaction rate, the temperature has an indirect effect modifying the solubility of gypsum [150], which could also play a role in this phenomenon.

From these results, it is obvious that the careful control of the experimental conditions is essential when planning the operational setup for industrial applications: the employed parameters must be tuned for every experimental site specifically.

Beside the external factors, the chemical composition of the matrix is also an important issue. In the mine drainages mentioned previously, a variety of metal ions are present, which can influence the precipitation kinetics of gypsum even in minuscule amounts, as discussed in section 2.2.2. Most of the metal ions should be removed in the first neutralization step as hydroxide precipitates, but still it is advised to perform tests to detect or determine them in the reaction mixture. Another type of impurities are organic molecules, which can come from either reactant. As shown earlier in section 2.2.3., different molecules can have different effects on the reaction. Some of these can be beneficial for the reaction by inhibiting the gypsum precipitation. On the other hand, they could interact in many ways with the additive and the precipitants causing novel inconveniences. The main reason behind the use of $Ca(OH)_2$ of natural source was to test if the precipitations can be separated even under near to industrial circumstances.

5.3.2. Analysis of the precipitates and the effect of washing

To characterize the different solids precipitating from the reactions, they had to be separated from the reaction mixture and each other. The process is discussed in detail in section 4.3.3. and presented in Figure 5. Studying the precipitates, it was found that in the initially filtered $Mg(OH)_2$ there was always some gypsum impurity present. The reason behind it is probably the inefficient filtration process, where the filtering cake often broke, hence some of the mother liquor (still supersaturated with respect to gypsum) remained on

the solid samples, and the gypsum precipitated during the drying process. To get rid of the gypsum in the samples, the samples were washed. After several experiments, it was found that the optimal washing volume was three-four times the volume of the withdrawn sample, using purified water. The composition of the solids was studied by XRD, the diffractograms are shown in Figure 27.

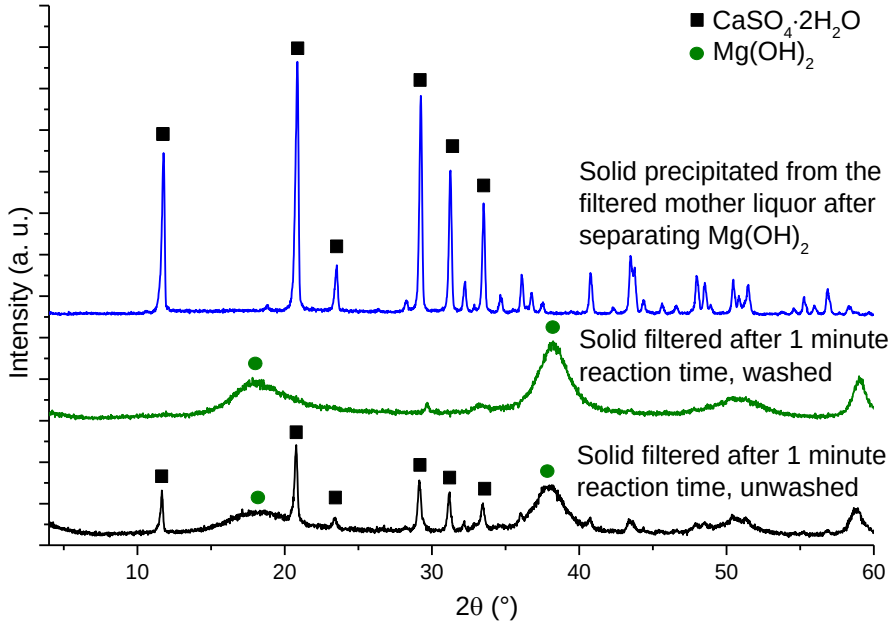

Figure 27. Diffractograms of the separated, precipitated solids; the main reflections were identified using the JCPDS database ($CaSO_4 \cdot 2H_2O$: # 21-0816 and $Mg(OH)_2$: # 84-2164). Washing of $Mg(OH)_2$ was carried out using purified water, four times the volume of withdrawn sample.

Magnesium hydroxide, without sufficient ageing, usually precipitates in the form of almost completely amorphous, poorly defined crystals resulting in wide, low-intensity reflections on the diffractograms. It can be seen that the high supersaturation and quick sampling led to the precipitation of such solids in our reactions. In contrast, the reflections of gypsum are sharp and intense making it easy to identify in the solids even in small amounts. Carrying out the washing process proposed, the reflections of gypsum disappeared suggesting that it was removed from the samples successfully.

The XRD data from several repeated reactions suggested that the washing of the initial solid was necessary, to end up with reasonably pure magnesium hydroxide. This led to the investigation of washing effects in reactions with various initial reactant concentrations. In parallel, the optimal time window for the initial filtration was also tested by taking samples at different reaction times from the reaction presented earlier in Figure 24. The washing

procedure was the same for every sample, purified water of four times the volume of the withdrawn sample was used. The results of these experiments are summarized in Table 5.

Table 5. Gypsum content in the washed, precipitated solids (according to XRD measurements) taken at given times in the $MgSO_4 + Ca(OH)_2 + 2\ H_2O \rightarrow \underline{Mg(OH)_2} + \underline{CaSO_4 \cdot 2H_2O}$ reaction carried out with varying initial reactant concentrations, while keeping the reactant-to-additive ratio constant (molar ratio of Ca:Mg:Citric acid = 0.1:0.1:0.0015)

Sample taken after	**Initial reactant concentration**		
	0.1 M	0.125 M	0.15 M
1 min	No gypsum present	No gypsum present	Gypsum present
5 min	-	Small amount of gypsum present	Gypsum present
10 min	No gypsum present	Gypsum present	Gypsum present
20 min	Gypsum present	Gypsum present	-

The time-window where the gypsum can be removed efficiently decreases rapidly with increasing reactant concentration. Besides the higher supersaturation, the larger amount of solids present also represents a challenge, since this makes the filtration process longer by thickening the filtration cake.

To observe the properties of $Mg(OH)_2$ in more detail, the morphologies of the unwashed and washed solids were studied by capturing their SEM images. The pictures are shown in Figure 28.

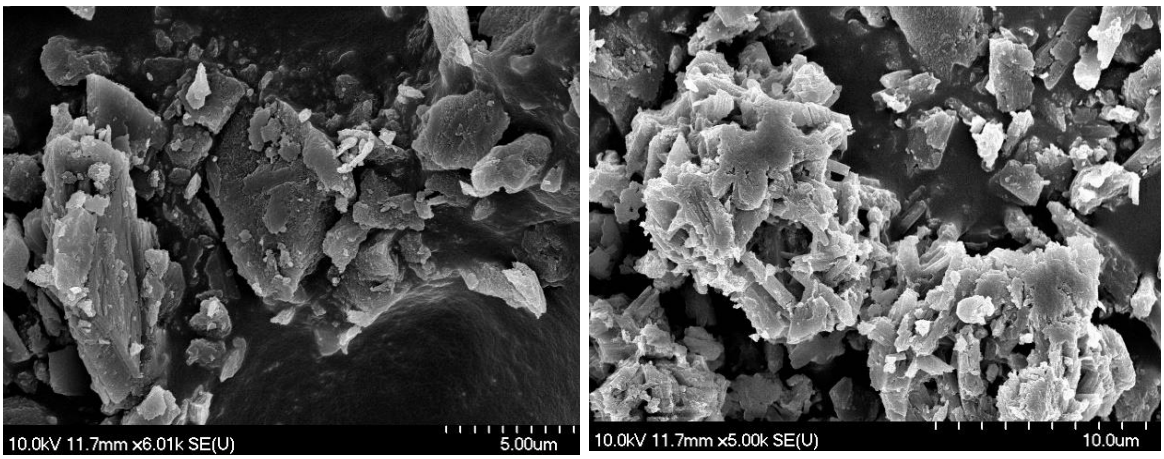

A **B**

Figure 28. SEM images of the precipitated $Mg(OH)_2$ **A**: washed sample (does not contain gypsum according to XRD) and **B**: unwashed sample (some gypsum present according to XRD)

Looking at the SEM images of the samples, no observable morphology can be seen, no regular crystal shapes can be found. This confirms our earlier statement that magnesium

hydroxide is formed in close to amorphous particles. The difference between the two samples is that the solids containing gypsum has small bumps and spikes on its surfaces and around the edges indicating that the gypsum precipitated on the surface of the magnesium hydroxide. To look at it in more detail, SEM-EDX measurements were carried out on the same samples. The results of the washed $Mg(OH)_2$ samples confirmed that they were practically calcium-free (the Ca concentration was estimated less than 1%). In the unwashed samples, this value was much higher, therefore the elemental map of the samples was registered to determine the distribution of the two elements (Figure 29).

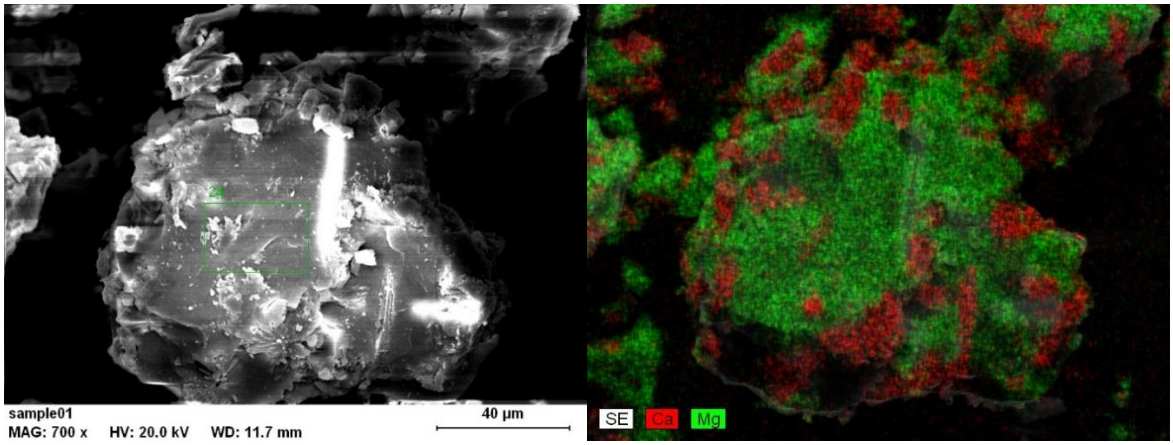

Figure 29. A: SEM-EDX picture and **B:** elemental map of a representative unwashed $Mg(OH)_2$ precipitate

On the elemental map one can see that the two solids are located separately, and the gypsum precipitated on the surface of $Mg(OH)_2$.

5.3.3. The location of citrate ions after the completion of both precipitation reactions

Determining the location of citrate after the completion of both precipitation processes is essential for economic and environmental reasons. The citrate content of the solids can alter their usability in various fields, which affects the cost-efficiency of the process.

The first step of locating citrate was the investigation of the filtered mother liquor by UV spectroscopy, after both precipitation reactions finished. The aim was to identify citrate groups through the band of C=O double bond adsorption in the 200-220 nm region. However, because quicklime of natural source was used in our reactions, some UV active impurities, most probably Fe(III), were present in the solution, which made the correct interpretation of these spectra impossible. Therefore, the further investigation of the separated fluids (final filtrate and washing fluid) and solids became necessary.

In the next step, four samples were prepared for HPLC measurements as described in section 4.3.3. The samples were washed $Mg(OH)_2$, separated $CaSO_4 \cdot 2H_2O$ (both digested in the eluent, 0.01 M sulfuric acid), the washing fluid of $Mg(OH)_2$ and the filtrate after the end of both precipitation reactions. Since the prepared samples had to be diluted for the measurements to avoid the precipitation of gypsum at higher pressure, the concentration of citric acid dropped close to the detection limit of the measuring equipment, therefore exact concentration could not be determined. The result of the measurements suggested that a portion of the citrate resided on the surface of the precipitated $Mg(OH)_2$, and the rest of it remained in the mother liquor inhibiting the precipitation of gypsum. In the samples of the digested gypsum and washing fluid, no sign of citric acid was detectable.

To confirm these findings, FT-IR measurements were carried out on the solids precipitated. To get a reference, an identical reaction was carried out in the absence of citric acid, and the solids were separated with exactly the same method. Without inhibitor, the precipitation of gypsum commences very early, therefore in these samples the gypsum impurity could not be washed out of the magnesium hydroxide samples. The comparison of the FT-IR spectra is presented in Figure 30.

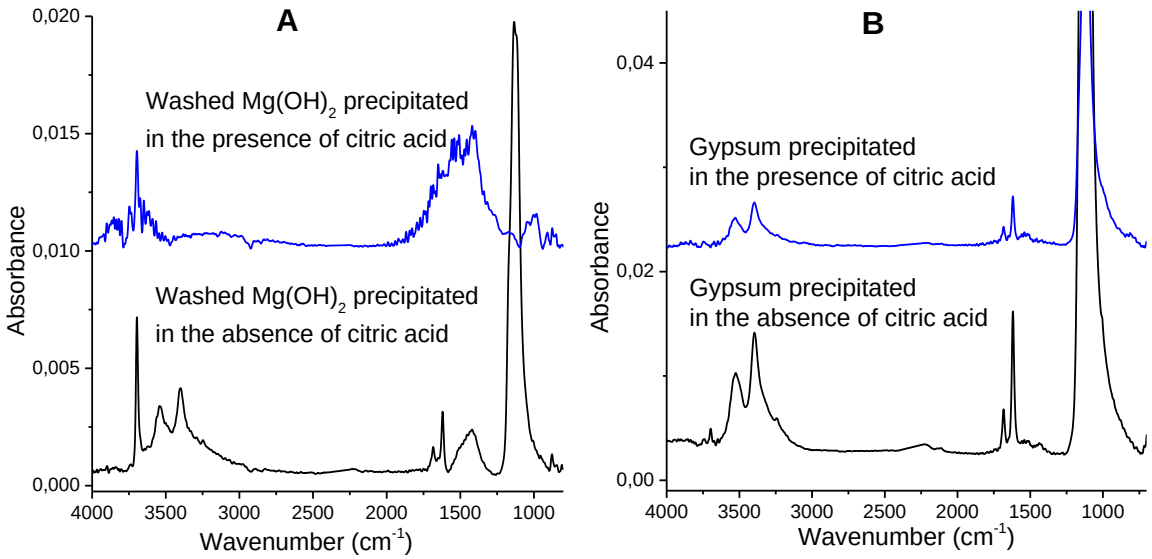

Figure 30. FT-IR spectra of the precipitated (A): $Mg(OH)_2$ and (B): $CaSO_4 \cdot 2H_2O$ in the presence of citrate ion (upper spectra) and those in the absence of the inhibitor (lower spectra)

In the spectra of the gypsum samples (Figure 29B), the characteristic peaks of $CaSO_4 \cdot 2H_2O$ can only be seen. In the practically identical spectra, only the typical vibrations of sulfate and crystalline water are present: the intense peaks around 1100-1200 cm^{-1} are the

signals of $\nu_3(SO_4)$ vibrations, the sharp peaks of the ν_2 vibrations of crystalline water are at 1620 and 1680 cm^{-1}, and the peaks standing out from the broad band in the 3000-3600 cm^{-1} correspond to the stretching mode of water [145]. On the other hand, the spectra of the magnesium hydroxides (Figure 29A) are noticeably different. The spectra of the solid precipitating from the reaction in the absence of citric acid is the combination of the spectra of $CaSO_4 \cdot 2H_2O$ and $Mg(OH)_2$. Beside the signals described above, a sharp peak appears at 3700 cm^{-1}, which is the signal of the stretching band of structural OH groups in $Mg(OH)_2$ [150]. There is also a broad band in the 1400-1600 cm^{-1} region corresponding to the bending vibration of the adsorbed water [151]. In the spectra of the $Mg(OH)_2$ precipitated in the presence of citric acid, there are no observable signs of gypsum. Also, some of the signs belonging to $Mg(OH)_2$ are partly masked by new bands appearing in the 1400-2000 cm^{-1} region and above 3500 cm^{-1}. On the basis of literature data [152, 153], these are the absorbance bands of citrate either in the form of magnesium or calcium salt. This way the minuscule amount of calcium found by SEM-EDX in the solids can also be explained. The citrate is probably bound to the surface of the $Mg(OH)_2$, and some of the calcium is taken with it to compensate the charge of the adsorbed citrate.

These results confirm our earlier assumption that citrate is partly bound by $Mg(OH)_2$, which is a possible explanation for the decreased inhibiting efficiency compared to the single-precipitate reaction. The phenomenon effectively removes some of the inhibitor from the reaction, thus only the remaining amount can retard the precipitation of gypsum. This must be taken into account, when the initial reactant concentration is increased, since the excess $Mg(OH)_2$ will bind more of the additive decreasing the efficiency of the inhibition.

These findings are promising regarding the possible industrialization of the process, since both the precipitated magnesium hydroxide and the final filtrate can be potentially recycled reducing the amount of waste produced, and thus the cost of the process. The $Mg(OH)_2$ should be efficient in the first step of the neutralization of acidic wastewaters, while the filtrate can be used to make up the neutralizing solids preparing the used slurries.

New scientific results derived from the findings described in section 5.3.:

T6. By inhibiting the gypsum crystallization with citrate ions, the reaction conditions for the *in situ* separation of $Mg(OH)_2$ and $CaSO_4 \cdot 2H_2O$ precipitates were optimized for the first time.

T7. The location of the citrate ions after the completion of the precipitation of both solid phases was determined, and it was shown that they were split between the $Mg(OH)_2$ and the final filtrate. With this finding it was demonstrated that the citrate additive was reusable in practical applications.

6. Summary and outlook

Kinetics of gypsum precipitation

In the first part of our work, the kinetics of gypsum ($CaSO_4 \cdot 2H_2O$) precipitation was studied during the stoichiometric reaction of sodium sulfate (Na_2SO_4) and calcium chloride ($CaCl_2$) in the absence of any further electrolyte or organic additive. The reaction was carried out with systematically varied initial reactant concentrations covering the whole experimentally available concentration range. The kinetics of the reactions was followed with a number of techniques (conductivity, potentiometry using Ca-ISE, ICP-OES) and the results obtained were compared. From the *in situ* techniques, the conductivity proved to be more robust over the whole concentration range, while the response of Ca-ISE legged behind in faster reactions.

The composition of the precipitates was studied by XRD, and the only identifiable phase was gypsum. The samples crystallized in rod- or needle-shaped crystals, but their sizes were polydisperse, since the particles were often broken, probably due to the high agitation speed.

The collected data of conductometric measurements were used to establish a kinetic model capable of describing comprehensively the nucleation and crystal growth processes of gypsum over a wide concentration range. The influence of the wall-effect on the reaction kinetics was found to be negligible. The necessary calculations were made with the ChemMech program package. During the calculations, the effect of the changing ionic strength was considered, both the dependence of the rate constants and its effect on the equivalent molar conductivity of the species present were taken into account. The inclusion of the ion-pair $CaSO_{4(aq)}$ was necessary for the model to work well in the whole concentration range. The results of the simultaneous fitting of the calculated data on the measured points implies that the suggested kinetic model is capable of describing the precipitation reaction over the whole experimentally available concentration range.

Effects and limitations of citric acid as an inhibitor in gypsum precipitation

The effects of citric acid on the precipitation of gypsum from highly supersaturated solutions was investigated in the stoichiometric reaction between $NaSO_4$ and $CaCl_2$. The reactions were monitored by conductometric measurements. The relatively high initial concentration and agitation rates were set to test the limitations of citric acid as an inhibitor. Investigating the effect of pH, it was found that the efficiency of inhibition was slowly decreasing under pH 5, and sharply dropped under pH 4 due to the protonation of the

carboxylic groups of citrate ions. Between pH 5 and 10, the reaction kinetics did not change significantly. The effect of citrate concentration was also studied, and it was found that the increase of the additive concentration did not increase the induction time proportionally; the inhibiting efficiency becomes constant from around 3 mM citrate concentration, probably due to the saturation of the gypsum surfaces, to which the additive can be bound. The efficiency of the inhibition is impressive, and considering the low cost and small environmental effect of the additive, it could be a promising candidate for many practical applications.

The effects of citrate inhibition on the precipitate were also investigated; the only identifiable solid was gypsum. It was observed on the XRD patterns of the samples that the intensities of the largest peaks decreased (both absolutely and compared to the other reflections) with the increasing inhibiting effect. This implied that the morphology of the crystal also changes, the rod- or needle-like shaped crystals in the absence of inhibitor changed to rhomboid and plate-like shapes in the presence of citrate ions.

Studying the UV spectra of the filtrate of the reaction mixtures after the reactions and the IR spectra of the filtered gypsum it was found that the citrate was not incorporated in the solid in detectable amounts. This is also promising regarding the possible reusability of the inhibitor.

To test the inhibiting efficiency of citric acid and citrate in processes involving solution mimicking seawater, the precipitation of gypsum was carried out in the presence of 1 M NaCl as background electrolyte. Since the solubility of gypsum is increased at higher ionic strength, the reaction rate was slower, hence the inhibiting efficiency of the same amount of citrate ion is much better. The high background conductivity made conductometric measurements impossible, but the slower reaction rate allowed us to apply Ca-ISE to follow the reaction.

Studying the solids precipitating from these reactions, similar tendencies were observed on the XRD patterns, but the differences were not so large as found in systems of low ionic strength. The morphology of the solids also changed; however, beside some rhomboid and plate shapes, the majority of the crystals formed short rods.

Differential precipitation of $Mg(OH)_2$ from $CaSO_4 \cdot 2H_2O$ in presence of citrate

During the scouting experiments, several potential inhibitors were tested in two reactions to withhold the precipitation of gypsum. In the stoichiometric reaction of Na_2SO_4 and $CaCl_2$, three of them (citrate, poly(acrylate) and DTPMP) appeared to be the most

promising. Those were tried in the stoichiometric reaction of $MgSO_4$ and $Ca(OH)_2$, the latter made from lime of natural source. In these reactions, only the citrate was found to keep a considerable fraction of its inhibiting efficiency, therefore it was used in the experiments to follow.

The *in situ* separation of the precipitation of $Mg(OH)_2$ and $CaSO_4 \cdot 2H_2O$ by the inhibition of the latter with citrate was carried out investigating the effects of the systematically varied experimental conditions. The effects of initial reactant concentration, citrate concentration and temperature were studied. It was found that these factors can compensate the effects of each other, and must be considered specifically for every individual application.

Studying the solids precipitating, it was found that the washing of the samples was necessary to get $Mg(OH)_2$ in the desired purity. The optimal amount was found 3-4 times the volume of the taken reaction slurry using purified water. The morphology of the precipitated $Mg(OH)_2$ was found to be almost amorphous, no identifiable shapes were seen on the SEM images. The SEM-EDX measurements suggested that the washed $Mg(OH)_2$ samples only contained calcium in less than 1 atomic %. The gypsum in the unwashed samples was crystallized on the surface of the $Mg(OH)_2$. The results suggest that the separation of the precipitation reactions is possible with careful planning, and can be used to optimize the neutralization process of acidic wastewater treatment, and it can also become useful in desalination processes.

To locate the citrate after the completion of both reaction, HPLC measurements were carried out on the fluid (filtrate and washing fluid) and digested solid ($Mg(OH)_2$ and $CaSO_4 \cdot 2H_2O$) samples. The results suggested that a portion of citrate was bound by the $Mg(OH)_2$, and some remained in the mother liquor inhibiting the gypsum precipitation. These results were confirmed by the IR spectra of the solids. In the spectrum of $Mg(OH)_2$ precipitated in presence of citrate, typical peaks of calcium or magnesium citrate can be found, while the spectra of the separated gypsum samples show only the signs of $CaSO_4 \cdot 2H_2O$. This implies that some of the citrate is bound on the surface of $Mg(OH)_2$ and if needed, some calcium ions are also bound to compensate the negative charge of citrate. The results imply that both $Mg(OH)_2$ and citrate can be recycled in the neutralization process, which improves the economic viability of the neutralization process. Considering also that citrate is a “green” additive, the environmental strain of the process would also decrease.

7. References

[1] Mucskai L., Ed.: Podhorányi Gy. Kristályosítás *Műszaki könyvkiadó, Budapest* **1971**

[2] Mullin J. W. Crystallization *Butterworth-Heineman, Oxford* **2001**

[3] Ed.: Myerson A. S. Handbook of crystallization *Elsevier Science & Technology Books* **2001**

[4] Ed.: Beckmann W. Crystallization: Basic Concepts and Industrial Applications *Wiley-VCH Verlag GmbH & Co. KGaA* **2013**

[5] Davies C. W. Ion Association *London: Butterworths* **1962** 37–53.

[6] Miers H. A., Isaak F. The spontaneous crystallisation of binary mixtures *P. Roy. Soc. A-Math. Phy.* **1907** *79* 322–351

[7] Young S. W. Mechanical stimulus to crystallization in super-cooled liquids *J. Am. Chem. Soc.* **1911** *33* 148–162

[8] Gibbs J. W. Collected works of J. Willard Gibbs *Yale University Press, New Haven* **1948**

[9] Frank F. C. The influence of dislocations on crystal growth *Discuss. Faraday Soc.* **1949** *5* 48–54

[10] Burton W. K., Cabrera N., Frank F. C. The growth of crystals and the equilibrium structure of their surfaces *Philos. T. Roy. Soc. A* **1951** *243* 299–358

[11] Frank F. C. On the kinematic theory of crystal growth and dissolution processes, II *Z. Phys. Chem. Neue Fol.* **1972** *77* 84–92

[12] van der Eerden J. P., Bennema P., Cherepanova T. A. Survey of Monte Carlo simulations of crystal surfaces and crystal growth *Prog. Cryst. Growth Ch.* **1978** *1* 219–254

[13] Freyer D., Voigt W. Crystallization and phase stability of $CaSO_4$ and $CaSO_4$ – based salts *Monatsh. Chem.* **2003** *134* 693–719

[14] Alimi F., Tlili M. M., BenAmora M., Maurin G., Gabrielli C. Effect of magnetic water treatment on calcium carbonate precipitation: Influence of the pipe material *Chem. Eng. Process.* **2009** *48* 1327–1332

[15] Hoang T. A., H. Ming Ang H., Rohl A. L. Effects of temperature on the scaling of calcium sulphate in pipes *Powder Technol.* **2007** *179* 31–37

[16] Hoang T. A., H. Ming Ang H., Rohl A. L. Effects of process parameters on gypsum scale formation in pipes *Chem. Eng. Technol.* **2011** *34* 1003–1009

[17] Hasson D., Avriel M., Resnick W., RozenmanT., Windreich S. Mechanism of calcium carbonate scale deposition on heat-transfer surfaces *Ind. Eng. Chem. Fundamen.* **1968** *7* 59–65

[18] Watkinson A. P., Martinez O. Scaling of heat exchanger tubes by calcium carbonate *J. Heat Transfer* **1975** *97* 504–508

[19] Hasson D., Zahavi J. Mechanism of calcium sulfate scale deposition on heat transfer surfaces *Ind. Eng. Chem. Fundamen.* **1970** *9* 1–10

[20] Shen J., Crosby C. C. Insight into strontium and calcium sulfate scaling mechanisms in a wet producer *J. Petrol. Technol.* **1983** *35* 1249–1255

[21] Oddo J. E., M.B. Tomson M. B. Why scale forms in the oil field and methods to predict it *SPE Prod. Facil.* **1994** *9* 47–54

[22] Binmerdhah A. B., Azam A., Yassin M. Study of scale formation due to incompatible water *J. Teknol.* **2008** *49* 9–26
[23] Brusilovsky M., Borden J., Hasson D. Flux decline due to gypsum precipitation on RO membranes *Desalination* **1992** *86* 187–222
[24] Rahman F. Calcium sulfate precipitation studies with scale inhibitors for reverse osmosis desalination *Desalination* **2013** *319* 79–84
[25] Abdel-Aal E. A., Abdel-Ghafar H. M., El Anadouli B. E. New findings about nucleation and crystal growth of reverse osmosis desalination scales with and without inhibitor *Cryst. Growth Des.* **2015** *15* 5133–5137
[26] Gilbert R. L. Jr. Crystallization of Gypsum in Wet Process Phosphoric Acid *Ind. Eng. Chem. Process Des. Dev.* **1966** *5* 388–391
[27] Kruger A., Focke W. W., Kwela Z., Fowles R. Effect of ionic impurities on the crystallization of gypsum in wet-process phosphoric acid *Ind. Eng. Chem. Res.* **2001** *40* 1364–1369
[28] Rashad M. M., Mahmoud M. H. H., Ibrahim I. A., Abdel-Aal E. A. Crystallization of calcium sulfate dihydrate under simulated conditions of phosphoric acid production in the presence of aluminum and magnesium ions *J. Cryst. Growth* **2004** *267* 372–379
[29] Lancia A., Musmarra D., Prisciandaro M., Tammaroa M. Catalytic oxidation of calcium bisulfite in the wet limestone–gypsum flue gas desulfurization process *Chem. Eng Sci.* **1999** *54* 3019–3026
[30] Neveux T., Le Moullec Y. Wet industrial flu gas desulfurization unit: Model development and validation on industrial data *Ind. Eng. Chem. Res.* **2011** *50* 7579–7592
[31] Dou B., Pan W., Jin Q., Wang W., Li Y. Prediction of SO2 removal efficiency for wet flue gas desulfurization *Energ. Convers. Manage.* **2009** 50 2547–2553
[32] Kuyucak N., Sheremata T. Lime neutralization process for treating acidic waters *United States patent* **1995** patent number: 5,427,691
[33] Gominšek T., Lubej A., Pohar C. Continuous precipitation of calcium sulfate dihydrate from waste sulfuric acid and lime *J. Chem. Technol. Biot.* **2005** *80* 939–947
[34] Zanin, M.; Lambert, H.; du Plessis, C. Lime Use and Functionality in Sulphide Mineral Flotation: A Review *Miner. Eng.* **2019** *143* 105922
[35] Schierholtz O. J. The crystallization of calcium sulphate dihydrate *Can. J. Chem.* **1958** *36* 1057–1063
[36] McCartney E. R., Alexander A. E. The effect of additives upon the process of crystallization I. Crystallization of calcium sulfate *J. Colloid Sci.* **1958** *13* 383–396
[37] Liu S. T., Nancollas G. H. The kinetics of crystal growth of calcium sulfate dihydrate *J. Cryst. Growth* **1970** *6* 281–289
[38] Nancollas G. H., Reddy M. M., Tsai F. Calcium sulfate dihydrate crystal growth in aqueous solution at elevated temperatures *J. Cryst. Growth* **1973** *20* 125–134
[39] Christoffersen J., Christoffersen M. R., van Rosmalen G. M., Marchée W. G. J. The affinity of crystal groeth and dissolution in aqueous solution with special reference to calcium sulphate dihydrate *J. Cryst. Growth* **1979** *47* 607–612

[40] Van Rosmalen G. M., Daudey P. J., Marchée W. G. J. An analysis of growth experiments of gypsum crystals in suspension *J. Cryst. Growth* **1981** *52* 801–811
[41] Christoffersen J., Christoffersen M. R., Weijnen M. P. C., van Rosmalen G. M. crystal growth of calcium sulphate at low supersaturation *J. Cryst. Growth* **1982** *58* 585–595
[42] Brandse W. P., van Rosmalen G. M., Brouwer G. The influence of sodium chloride on the crystallization of gypsum *J. Inorg. Nucl. Chem.* **1977** *39* 2007–2010
[43] Smith B. R., Sweet F. The crystallization of calcium sulfate dihydrate *J. Coll. Interf. Sci.* **1971** *37* 612–618
[44] Witkamp G. J., van der Eerden J. P., van Rosmalen G. M. Growth of gypsum I. Kinetics *J. Cryst. Growth* **1990** *102* 281–289
[45] de Meer S., Spiers S. J., Peach C. J. Kinetics of precipitation of gypsum and implications for pressure-solution creep *J. Geol. Soc. London* **2000** *157* 269–281
[46] Amathieu L., Boistelle R. Crystallization kinetics of gypsum from dense suspension of hemihydrate in water *J. Cryst. Growth* **1988** *88* 183–192
[47] Singh N. B., Middendorf B. Calcium sulphate hemihydrate hydration leading to gypsum crystallization *Prog. Cryst. Growth Ch.* **2007** *53* 57–77
[48] Packter A. The precipitation of calcium sulphate from aqueous solution *J. Cryst. Growth* **1974** *21* 191–194
[49] Alimi F., Elfil H., Gadrib A. Kinetics of the precipitation of calcium sulfate dihydrate in a desalination unit *Desalination* **2003** *157* 9–16
[50] Alimi F., Gadrib A. Kinetics and morphology of formed gypsum *Desalination* **2004** *166* 427–434
[51] Klepetsanis P. G., Koutsoukos P. G. Precipitation of calcium sulfate dihydrate at constant calcium activity *J. Cryst. Growth.* **1989** *98* 480–486
[52] Klepetsanis P. G., Koutsoukos P. G. Spontaneous precipitation of calcium sulfate at conditions of sustained supersaturation *J. Coll. Interf. Sci.* **1991** *143* 299–308
[53] Klepetsanis P. G., Dalas E., Koutsoukos P. G. Role of temperature in the spontaneous precipitation of calcium sulfate dihydrate *Langmuir* **1999** *15* 1534–1540
[54] Lancia A., Musmarra D., Prisciandaro M. Measuring induction period for calcium sulfate dihydrate precipitation *AIChE J.* **1999** *45* 390–397
[55] Hina A., Nancollas G. H. Precipitation and dissolution of alkaline earth sulfates: kinetics and surface energy *Rev. Mineral. Geochem.* **2000** *40* 277–301
[56] Rendel P. M., Gavrieli I., Wolff-Boenisch D., Ganor J. Towards establishing a combined rate law of nucleation and crystal growth – The case study of gypsum precipitation *J. Cryst. Growth.* **2018** *485* 28–40
[57] Linnikov O. D. Investigation of the initial period of sulphate scale formation Part 1. Kinetics and mechanism of calcium sulphate surface nucleation at its crystallization on a heat-exchange surface *Desalination* **1999** *122* 1–14
[58] Linnikov O. D. Investigation of the initial period of sulphate scale formation Part 2. Kinetics of calcium sulphate crystal growth at its crystallization on a heat-exchange surface *Desalination* **2000** *128* 35–46

[59] He S., Oddo J. E., Tomson M. B. The nucleation kinetics of calcium sulfate dihydrate in NaCl solutions up to 6 m and 90°C *J. Coll. Interf. Sci.* **1994** *162* 297–303

[60] Prisciandaro M., Lancia A., Musmarra D. Calcium Sulfate Dihydrate Nucleation in the Presence of Calcium and Sodium Chloride Salts *Ind. Eng. Chem. Res.* **2001** *40* 2335–2339

[61] Reznik I. J., Gavrieli I., Ganor J. Kinetics of gypsum nucleation and crystal growth from Dead Sea brine *Geochim. Cosmochim. Ac.* **2009** *73* 6218–6230

[62] Reznik I. J., Gavrieli I., Antler G., Ganor J. Kinetics of gypsum crystal growth from high ionic strength solutions: A case study of Dead Sea – seawater mixtures *Geochim. Cosmochim. Ac.* **2011** *75* 2187–2199

[63] Dydo P., Turek M., Ciba J., Wandachowicz K., Misztal J. The nucleation kinetic aspects of gypsum nanofiltration membrane scaling *Desalination* **2004** *164* 41–52

[64] Uchymiak M., Lyster E., Glater J., Cohen Y. Kinetics of gypsum crystal growth on a reverse osmosis membrane *J. Membrane Sci.* **2008** *314* 163–172

[65] Cetin E., Eroglu I., Özkar S. Kinetics of gypsum formation and growth during the dissolution of colemanite in sulfuric acid *J. Cryst. Growth.* **2001** *231* 559–567

[66] Abdel-Aal E. A., Rashad M. M., El-Shall H. Crystallization of calcium sulfate dihydrate at different supersaturation ratios and different free sulfate concentrations *Cryst. Resol. Technol.* **2004** *39* 313–321

[67] Wang Y. W., Kim Y. Y., Christenson H. K., Meldrum F. C. A new precipitation pathway for calcium sulfate dihydrate (gypsum) *via* amorphous and hemihydrate intermediates *Chem. Commun.* **2012** *48* 504–506

[68] Van Driessche A. E. S., Benning L. G., Rodriguez-Blanco J. D., Ossorio M., Bots P., García-Ruiz J. M. The role and implications of bassanite as a stable precursor phase to gypsum precipitation *Science* **2012** *336* 69–72

[69] Stawski T. M., van Driessche A. E. S., Ossorio M., Rodriguez-Blanco J. D., Besselink R., Benning L. G. Formation of calcium sulfate through the aggregation of sub-3 nanometre primary species *Nat. Commun.* **2016** *7* 1–9

[70] Wollmann G., Voigt W. Solubility of gypsum in MSO4 solutions (M) Mg, Mn, Co, Ni, Cu, Zn) at 298.15 K and 313.15 K *J. Chem. Eng. Data* **2008** *53* 1375–1380

[71] Hamdona S. K., Nessim R. B., Hamza S. M. Spontaneous precipitation of calcium sulphate dihydrate in the presence of some metal ions *Desalination* **1993** *94* 69–80

[72] Hamdona S. K., Al Hadad U. A. Crystallization of calcium sulfate dihydrate in the presence of some metal ions *J. Cryst. Growth* **2007** *299* 146–151

[73] Gao X., Huo W., Zhong Y., Luo Z., Cen K., Ni M., Chen L. Effects of magnesium and ferric ions on crystallization of calcium sulfate dihydrate under the simulated conditions of wet flue-gas desulfurization *Chem. Res. Chinese U.* **2008** *24* 688–693

[74] Guan B., Yang L., Wu Z. Effect of Mg^{2+} ions on the nucleation kinetics of calcium sulfate in concentrated calcium chloride solutions *Ind. Eng. Chem. Res.* **2010** *49* 5569–5574

[75] Deng L., Zhang Y., Chen F., Cao S., You S., Liu Y., Zhang Y. Reactive crystallization of calcium sulfate dihydrate from acidic wastewater and lime *Chinese J. Chem. Eng.* **2013** *21* 1303–1312

[76] Ahmed S. B., Tlili M. M., Amami M., Amor M. B. Gypsum precipitation kinetics and solubility in the NaCl−$MgCl_2$−$CaSO_4$−H_2O system *Ind. Eng. Chem. Res.* **2014** *53* 9554−9560

[77] Rabizadeh T., Stawski T. M., Morgan D. J., Peacock C. L., Benning L. G. The effects of inorganic additives on the nucleation and growth kinetics of calcium sulfate dihydrate crystals *Cryst. Growth Des.* **2017** *17* 582−589

[78] Hamdonaa S. K., Al Hadad O. A. Influence of additives on the precipitation of gypsum in sodium chloride solutions *Desalination* **2008** *228* 277–286

[79] Witkamp G. J., van Rosmalen G. M. Growth of gypsum II. Incorporation of cadmium *J. Cryst. Growth* **1991** *108* 89–98

[80] Sayan P., Titiz-Sargut S., Avcı B. Effect of trace metals on reactive crystallization of gypsum *Cryst. Res. Technol.* **2007** *42* 961–970

[81] F. Adams J. F., Papangelakis V. G. Gypsum scale formation in continuous neutralization reactors *Can. Metall. Quart.* **2000** *39* 421–432

[82] de Vreugd C. H., Witkamp G. J., van Rosmalen G. M. Growth of gypsum III. Influence and incorporation of lanthanide and chromium ions *J. Cryst. Growth* **1994** *144* 70–78

[83] Shih W.-Y., Gao J., Rahardianto A., Glater J., Cohen Y., Gabelich C. J. Ranking of antiscalant performance for gypsum scale suppression in the presence of residual aluminum *Desalination* **2006** *196* 280–292

[84] Shih W.-Y., Albrecht K., Glater J., Cohen Y. A dual-probe approach for evaluation of gypsum crystallization in response to antiscalant treatment *Desalination* **2004** *169* 213–221

[85] Liu S. T., Nancollas G. H. A kinetic and morphological study of the seeded growth of calcium sulfate dihydrate in presence of additives *J. Coll. Interf. Sci.* **1975** *52* 593–601

[86] Klepetsanis P. G., Koutsoukos P. G. Kinetics of calcium sulfate formation in aqueous media: effect of organophosphorus compounds *J. Cryst. Growth* **1998** *193* 156–163

[87] Prisciandaro M., Olivieri E., Lancia A., Musmarra D. Gypsum precipitation from an aqueous solution in the presence of nitrilotrimethylenephosphonic acid *Ind. Eng. Chem. Res.* **2006** *45* 2070–2076

[88] Prisciandaro M., Olivieri E., Lancia A., Musmarra D. Gypsum scale control by nitrilotrimethylenephosphonic acid *Ind. Eng. Chem. Res.* **2009** *48* 10877–10883

[89] Akyol E., Öner M., Barouda E., Demadis K. D. Systematic structural determinants of the effects of tetraphosphonates on gypsum crystallization *Cryst. Growth Des.* **2009** *9* 5145–5154

[90] Prisciandaro M., Olivieri E., Lancia A., Musmarra D. PBTC as an antiscalant for gypsum precipitation: interfacial tension and activation energy estimation *Ind. Eng. Chem. Res.* **2012** *51* 12844−12851

[91] El-Shall H., Rashad M. M., Abdel-Aal E. A. Effect of phosphonate additive on crystallization of gypsum in phosphoric and sulfuric acid medium *Cryst. Res. Technol.* **2002** *37* 1264–1273

[92] Hoang T. A., Ming Ang H., Rohl A. L. Effects of organic additives on calcium sulfate scaling in pipes *Aust. J. Chem.* **2009** *62* 927–933

[93] Weijnen M. P. C., van Rosmalen G. M. The influence of various polyelectrolytes on the precipitation of gypsum *Desalination* **1985** *54* 239–261

[94] Lioliou M. G., Paraskeva C. A., Koutsoukos P. G., Payatakes A. C. Calcium sulfate precipitation in the presence of water-soluble polymers *J. Coll. Interf. Sci.* **2006** *303* 164–170

[95] Xue X., Fu C., Li N., Zheng F., Yang W., Yang X. Performance of a non-phosphorus antiscalant on inhibition of calcium-sulfate precipitation *Water Sci. Technol.* **2012** *66* 193–200

[96] Amjad Z. Gypsum scale formation on heated metal surfaces: The influence of polymer type and polymer stability on gypsum inhibition *Desalin. Water Treat.* **2013** *51* 4709–4718

[97] Amjad Z., Koutsoukos P. G. Evaluation of maleic acid based polymers as scale inhibitors and dispersants for industrial water applications *Desalination* **2014** *335* 55–63

[98] Feldmann T., Demopoulos G. P. Effects of crystal habit modifiers on the morphology of calcium sulfate dihydrate grown in strong $CaCl_2$-HCl solutions *J. Chem. Technol. Biotechnol.* **2014** *89* 1523–1533

[99] Popov K., Rudakova G., Larchenko V., Tusheva M., Kamagurov S., Dikareva J., Kovaleva N. A comparative performance evaluation of some novel "green" and traditional antiscalants in calcium sulfate scaling *Adv. Mater. Sci. Eng.* **2016** 7635329:1–11

[100] Rabizadeh T., Morgan D. J., Peacock C. L., Benning L. G. Effectiveness of green additives vs poly(acrylic acid) in inhibiting calcium sulfate dihydrate crystallization *Ind. Eng. Chem. Res.* **2019** *58* 1561−1569

[101] Benecke J., Rozova J., Ernst M. Anti-scale effects of select organic macromolecules on gypsum bulk and surface crystallization during reverse osmosis desalination *Sep. Purif. Technol.* **2018** *198* 68–78

[102] Mahmoud M. H. H., Rashad M. M., Ibrahim I. A., Abdel-Aal E. A. Crystal modification of calcium sulfate dihydrate in the presence of some surface-active agents *J. Coll. Interf. Sci.* **2004** *270* 99–105

[103] Badens E., Veesler S., Boistelle R. Crystallization of gypsum from hemihydrate in presence of additives *J. Cryst. Growth* **1999** *198/199* 704–709

[104] Rabizadeh T., Peacock C. L., Benning L. G. Carboxylic acids: effective inhibitors for calcium sulfate precipitation? *Mineral. Mag.* **2014** *78* 1465–1472

[105] Vellmer C., Middendorf B., Singh N. B. Hydration of α-hemihydrate in the presence of carboxylic acids *J. Therm. Anal. Calorim.* **2006** *86* 721–726

[106] Prisciandaro M., Lancia A., Musmarra D. The retarding effect of citric acid on calcium sulfate nucleation kinetics *Ind. Eng. Chem. Res.* **2003** *42* 6647–6652

[107] Prisciandaro M., Santucci A., Lancia A., Musmarra D. Role of citric acid in delaying gypsum precipitation *Can. J. Chem. Eng.* **2005** *83* 586–592

[108] Titiz-Sargut S., Sayan P., Avcı B. Influence of citric acid on calcium sulfate dihydrate crystallization in aqueous media *Cryst. Res. Technol.* **2007** *42* 119–126

[109] Titiz-Sargut S., Sayan P., Kiran B. Gypsum crystallization in the presence of Cr^{3+} and citric acid *Chem. Eng. Technol.* **2010** *33* 804–811

[110] Qu J., Peng J., Li B. Effect of citric acid on the crystal morphology of gypsum and its action mechanism *Adv. Mat. Res.* **2011** *250* 321–326

[111] Rashad M. M., Mahmoud M. H. H., Ibrahim I. A., Abdel-Aal E. A. Effect of citric acid and 1,2-dihydroxybenzene 3,5-disulfonic acid on crystallization of calcium sulfate dihydrate under simulated conditions of phosphoric acid production *Cryst. Res. Technol.* **2005** *40* 741–747

[112] Lv L., Gao R., Yang J., Shen Z., Zhou Y., Lu J. Investigation of organic desulfurization additives affecting the calcium sulfate crystals formation. *Chem. Ind. Chem. Eng. Q.* **2017** *23* 161–167

[113] Ersen A., Smith A., Chotard T. Effect of malic and citric acid on the crystallisation of gypsum investigated by coupled acoustic emission and electrical conductivity techniques *J. Mater. Sci.* **2006** *41* 7210–7217

[114] Najafi Kani E., Nejan M., Allahverdi A. Investigating the relationship between heat of hydration and physico-mechanical properties of calcium sulfate hemihydrate in the presence of additives *Iran. J. Mater. Sci. Eng.* **2016** *13* 61–70

[115] Deng Y., Luo J., Zai D., Xuan L., Han Z., Dai C., Xu H., Feng M., He G. Study of the retarding mechanism of citric acid during gypsum particleboard manufacturing *Holzforschung* **2008** *62* 368–371

[116] Raharjo S., Muryanto S., Jamari J., Bayuseno A. P. Optimization of calcium sulfate precipitated in the laminar flow pipe through response surface modeling of temperature, Ca^{2+} concentration and citric acid additives *Orient. J. Chem.* **2016** *32* 3145–3154

[117] Tadros M. E., Mayes I. Linear growth rates of calcium sulfate dihydrate crystals in the presence of additives *J. Coll. Interf. Sci.* **1979** *72* 245–254

[118] Al-Sabbagh A., Widua J., Offermann H. Influence of different admixtures on the crystallization of calcium sulfate crystals *Chem. Eng. Comm.* **1996** *154* 133–145

[119] Chen W., Zhao W., Wu Y., Wang Y., Zhang B., Li F., Chen Q., Qi Z., Xu Z. Origin of gypsum growth habit difference as revealed by molecular conformations of surface-bound citrate and tartarate *Cryst. Eng. Comm.* **2018** *20* 3581–3589

[120] van der Voort E., Hartman P. The habit of gypsum and solvent interaction *J. Cryst. Growth* **1991** *112* 445–450

[121] Bologo V., Maree J. P., Zvindowanda C. M. Treatment of acid mine drainage using magnesium hydroxide *Proceedings of the International Mine Water Conference, Pretoria, South Africa* **2009** 19–23

[122] Ineich T., Degreve C., Karamoutsos S., du Plessis C. Utilization efficiency of lime consumption during magnesium sulfate precipitation *Hydrometallurgy* **2017** *173* 241-249

[123] Nie J., Yi S. Z. Neutralization of acid wastewater and magnesium hydroxide slurry from seawater electrolytic pretreatment *Adv. Mat. Res.* **2015** *1073* 949–954

[124] Carson R. C., Simandl J. Kinetics of magnesium hydroxide precipitation from seawater using slaked dolomite *Miner. Eng.* **1994** *7* 511–517

[125] Alamdari A., Rahimpour M. R., Esfandiari N., Nourafkan E. Kinetics of magnesium hydroxide precipitation from sea bittern *Chem. Eng. Process.* **2008** *47* 215–221

[126] Gong M. H., Johns M., Fridjonsson E., Heckley P. Magnesium Recovery from Desalination Brine *CEED Seminar Proceedings* **2018** 49–54

[127] Liu S. T., Nancollas G. H. The crystallization of magnesium hydroxide *Desalination* **1973** *12* 75–84

[128] Klein D. H., Smith M. D., Driy J.A. Homogeneous nucleation of magnesium hydroxide *Talanta* **1967** *14* 937–940

[129] Söhnel O., Mareček J. Precipitation of magnesium hydroxide *Krist. Tech.* **1978** *13* 253–262

[130] Chieng C., Nancollas G. H. The crystallization of magnesium hydroxide, a constant composition study *Desalination* **1982** *42* 209–219
[131] Yuan Q., Lu Z., Zhang P., Luo X., Ren X., Golden T. D. Study of the synthesis and crystallization kinetics of magnesium hydroxide *Mater. Chem. Phys.* **2015** *162* 734–742
[132] Walinsky S. W., Morton B. J. Chemistry of alkaline scale inhibition in seawater desalination by Flocon antiscalant 247 *Desalination* **1979** *31* 289–298
[133] Xu C., Wang F., Liu D., Chen W. Effect of additive EDTA on crystallization process of magnesium hydroxide precipitation *Chin. J. Chem. Eng.* **2010** *18* 761–766
[134] LebedevA. L., Kosorukov V. L. Gypsum solubility in water at 25°C *Geochem Int+* **2017** *55* 205–210
[135] Peintler G, ZITA(1989–2012) and ChemMech (2013–2019), A comprehensive program package for fitting parameters of chemical reaction mechanisms, versions 2.1–5.0, Department of Physical Chemistry, University of Szeged, Szeged, Hungary (1989–2019)
[136] Shedlovsky T., Brown A. S. The electrolytic conductivity of alkaline earth chlorides in water at 25° *J. Am. Chem. Soc.* **1934** *56* 1066–1071
[137] Benson G. C., Gordon A. R. The conductance of aqueous solutions of calcium chloride at temperatures from 15° to 45° C *J. Chem. Phys.* **1945** *13* 470–472
[138] Chambers J. F., Stokes J. M., Stokes R. H. Conductances of concentrated aqueous sodium and potassium chloride solutions at 25° *J. Phys. Chem.* **1956** *60* 985–986
[139] Sun I., Newman J. The electrical conductivity of aqueous solutions of calcium chloride *Lawrence Berkeley National Laboratory* **1970** (LBNL Report #: UCRL-19150)
[140] Isono T. Density, viscosity, and electrolytic conductivity of concentrated aqueous electrolyte solutions at several temperatures. Alkaline-earth chlorides, lanthanum chloride, sodium chloride, sodium nitrate, sodium bromide, potassium nitrate, potassium bromide, and cadmium nitrate *J. Chem. Eng. Data* **1984** *29* 45–52
[141] McCleskey R. B. Electrical conductivity of electrolytes found in natural waters from (5 to 90) °C *J. Chem. Eng. Data* **2011** *56* 317–327
[142] Chapman T. W., Newman J. A. compilation of selected thermodynamic and transport properties of binary electrolytes in aqueous solution *Lawrence Berkeley National Laboratory* **1968** (LBNL Report #: UCRL-17767)
[143] Ed.: Lide D. R. CRC handbook of chemistry and physics: a ready-reference book of chemical and physical data (84th ed.) *CRC press* **2003**
[144] du Plessis C., private communication
[145] Singh R.P., Yeboah Y.D., Pambid E.R., Debayle P. Stability Constant of the Calcium-Citrate(3-) Ion Pair Complex *J. Chem. Eng. Data* **1991** *36* 52-54
[146] Bensted J., Prakash S. Investigation of the calcium sulphate–water system by infrared spectroscopy *Nature* **1968** *219* 60–61
[147] Cameron F. K. Solubility of gypsum in aqueous solutions by sodium chloride *J. Phys. Chem.* **1901** *5* 556–576
[148] Bock E. On the solubility of anhydrous calcium sulphate and of gypsum in concentrated solutions of sodium chloride at 25 C, 30 C, 40 C, and 50 C *Can. J. Chem.* **1961** *39* 1746–1751

[149] Nicoleau L., Van Driessche A.E.S., Kellermeier M. *Cement Concrete Res.* **2019** *124* 105837

[150] Partridge E.P., White A.H. The solubility of calcium sulfate from 0 to 200 *J. Am. Chem. Soc.* **1929** *51* 360–370

[151] Wiley SpectraBase. SpectraBase Compound ID 7kH3z5zFF2C. Available online: https://spectrabase.com/ spectrum/9GqJIqcyzih (accessed on 17 July 2020)

[152] Wiley SpectraBase. SpectraBase Compound ID FXpCU14bzDK. Available online: https://spectrabase.com/ spectrum/Kof74u1OB3P (accessed on 17 July 2020)

[153] Chanfrau J. E. R., Álvarez L. M., Crespo A. B. Evaluation of calcium and magnesium citrate from Cuban dolomite. *Rev. Cuba. Farm.* **2014** *48* 636–645

Magyar nyelvű összefoglaló / Summary and outlook in Hungarian

Gipsz kristályosodásának kinetikája

Munkánk első részében a gipsz ($CaSO_4 \cdot 2H_2O$) kristályosodási reakciójának a kinetikáját tanulmányoztuk, nátrium-szulfát (Na_2SO_4) és kalcium-klorid ($CaCl_2$) sztöchiometrikus reakciójában. A kísérleteket háttérelektrolit vagy szerves adalék hozzáadása nélkül hajtottuk végre. A vizsgálatok során a reaktánsok kiindulási koncentrációját szisztematikusan változtattuk a teljes kísérletileg elérhető koncentráció-tartományban. A reakciók lefutását három különböző mérési módszerrel követtük (*in situ* vezetőképesség-méréssel és direkt potenciometriával Ca-ISE-ot alkalmazva, ill. *ex situ* ICP-OES technikával), melyek eredményeit összehasonlítottuk. Az *in situ* módszerek közül a vezetőképesség mérés bizonyult megbízhatónak a teljes koncentrációtartományban, a Ca-ISE válasza kissé késleltetett volt a gyorsabb reakciók követése során.

A keletkezett csapadékok összetételét XRD segítségével tanulmányoztuk; az egyetlen azonosítható kristályos fázis gipsz volt. A részecskék morfológiáját vizsgálva a gipszre jellemző tű vagy pálcika alakú kristályokat figyeltünk meg. A kristályok mérete meglehetősen nagy szórást mutatott, gyakran találhatók közöttük törött részecskék is, ami valószínűleg a viszonylag gyors kevertetés hatásának tudható be.

A vezetőképesség mérés eredményeit felhasználva felállítottunk egy kinetikai modellt, amely képes a gipsz nukleációját és a kristályok növekedését egyszerre leírni széles koncentrációtartományban. Megállapítottuk, hogy a falhatás elhanyagolható mértékben befolyásolja a reakciók kinetikáját. A kinetikai számításokat a ChemMech programcsomag segítségével végeztük el. A számítások során az ionerősség változását is figyelembe kellett vennünk, mivel a reakciósebességi együtthatók függenek tőle, valamint hatással van az egyes komponensek ekvivalens moláris vezetőképességére. A modell megfelelő működéséhez feltétlenül szükség volt a $CaSO_{4(aq)}$ ionpár keletkezésének figyelembe vételére. Az adatok együttes illesztése során tapasztalt kiváló egyezés a számolt és mért értékek között arra utal, hogy az általunk javasolt modell megfelelően képes leírni a gipsz kristályosodásának reakcióját a teljes kísérletileg elérhető koncentrációtartományban.

A citromsav hatásai és korlátai mint a gipsz kristályosodásának inhibitora

A citromsav hatásait gipsz magas túltelítettségű oldatokból való kristályosodására szintén a $NaSO_4$ és a $CaCl_2$ sztöchiometrikus reakciója során vizsgáltuk. A reakciókat

vezetőképesség méréssel követtük. Annak érdekében, hogy meg tudjuk vizsgálni a citromsav inhibítorként történő felhasználási lehetőségeit és korlátait, a reakciók végrehajtása során viszonylag magas kezdeti túltelítettséggel és kevertetési sebességgel dolgoztunk. A pH hatását vizsgálva azt találtuk, hogy az inhibíció hatásfoka pH 5 alatt lassan, majd pH 4 alatt drasztikusan csökken, a citrát-ion karboxilát-csoportjainak protonálódása miatt. A reakció kinetikája nem változott jelentősen pH 5 és 10 között. A citrát koncentrációjának hatását vizsgálva megfigyeltük, hogy az adalék koncentrációját növelve, az indukciós periódus növekedése azzal nem egyenesen arányos, 3 mM citrát-koncentráció felett a kristályosodási reakció nem lassult tovább. Ez valószínűleg annak tudható be, hogy a kialakuló és növekvő kristályok olyan felületei, melyeken a citrát képes megkötődni, telítődtek, így az inhibítor koncentrációjának további növelése már nem képes jelentősen lassítani azok növekedését. Az inhibíció mértéke még így is figyelemreméltó, különösen, ha megfontoljuk a citromsav alacsony árát és kis környezeti hatását ("zöld" adalék), mely szempontok miatt felhasználása különösen ígéretes lehet különféle gyakorlati, ipari folyamat során.

A citrát hozzáadásának csapadékra gyakorolt hatásait is megvizsgáltuk; itt is a gipsz volt az egyetlen azonosítható kristályos fázis a felvett diffraktogramok alapján. A mérések során azt tapasztaltuk, hogy az inhibíció mértékét növelve a legintenzívebb reflexiók intenzitása csökkent mind abszolút értékben, mind pedig a többi reflexióhoz képest. Ez arra utal, hogy a kiváló részecskék morfológiája jelentősen megváltozott. A SEM képek alapján a citrátmentes rendszerekből kivált részecskék tű, illetve pálcika alakúak, míg a citrát jelenlétében kiváló kristályok rombusz és lapka formájúak voltak.

A reakció után kapott szűrletek UV spektrumát és a szilárd minták IR spektrumát tanulmányozva megállapítottuk, hogy a citrát az oldatban marad, nem válik ki a gipsszel kimutatható mennyiségben. Ez az eredmény szintén ígéretes ipari szempontból, hiszen lehetővé teheti az adalék újrafelhasználását.

Annak érdekében, hogy megvizsgáljuk a citromsav hasznosságát tengervizet használó folyamatok során, a gipsz kristályosítási reakcióját a korábbiakhoz hasonlóan, de 1 M NaCl háttérelektrolit jelenlétében is végrehajtottuk. Mivel a gipsz oldhatósága ezekben a rendszerekben jelentősen megnövekszik, a reakció sebessége csökken, így a reakció lassítása is hatékonyabbá válik azonos mennyiségű adalék felhasználásával. Bár a háttérelektrolit viszonylag magas kiindulási vezetése lehetetlenné tette a vezetőképesség mérés alkalmazását, a lassúbb reakció követhetőnek bizonyult Ca-ISE-vel.

A kiváló csapadék vizsgálata során hasonló tendenciákat figyelhettünk meg, mint a háttérelektrolit nélküli rendszerekben. A minták diffraktogramjain a (0 2 0) és (1 3 0) reflexiók intenzitásának csökkenése itt is megfigyelhető, bár a különbségek jóval kisebbek voltak. A kristályok morfológiája is megváltozott az inhibíció hatására, azonban a gipsz citrát jelenlétében rombusz és lapka alakú kristályok mellett fő tömegben rövid, összenyomott pálcika alakot vett fel.

$Mg(OH)_2$ és $CaSO_4 \cdot 2H_2O$ kicsapódásának időbeli elválasztása citrát segítségével

Előkísérleteink során számos lehetséges inhibitort kipróbáltunk, annak érdekében, hogy lassítsuk vagy megakadályozzuk a gipsz kristályosodását. Na_2SO_4 és $CaCl_2$ sztöchiometrikus reakciója során három adalék (citrát, poly(akrilát), DTPMP) bizonyult megfelelőnek. Ezeket az adalékokat $MgSO_4$ és $Ca(OH)_2$ (az utóbbi természetes forrásból származó mészkőből előállítva) sztöchiometrikus reakciójában is teszteltük. A három adalék közül csupán a citrát tartotta meg hatékonyságának egy részét, míg a másik két anyag kifejezetten rosszul működött inhibítorként ebben a rendszerben. Emiatt a továbbiakban a $Mg(OH)_2$ és $CaSO_4 \cdot 2H_2O$ kristályosodásának *in situ* szétválasztásához adalékként citrátot alkalmaztunk a csapadékképzési reakciók szétválasztására, illetve az utóbbi leválásának lassítására.

A kísérletek során a reakciókörülményeket (reaktánsok kezdeti koncentrációja, adalék koncentrációja, hőmérséklet) szisztematikusan változtattuk, hogy megvizsgáljuk azok hatásait. Megállapítottuk, hogy ezek a paraméterek egymás hatásait kölcsönösen befolyásolják, de a megfelelő körülmények megválasztásával a reakciók megfelelő mértékben időben szétválaszthatókká válnak.

A kivált szilárd anyagokat vizsgálva azt tapasztaltuk, hogy a minták mosása mindenképp szükséges a kívánt tisztaságú $Mg(OH)_2$ előállításához. Desztillált vizet használva, a vett minta térfogatának három-négyszerese bizonyult optimálisnak a szennyező gipsz megfelelő kimosásához. A kivált $Mg(OH)_2$ nem rendelkezett jól látható morfológiával a SEM képek alapján. A SEM-EDX mérések szerint a megfelelően mosott $Mg(OH)_2$ minták kalciumot csupán kevesebb, mint egy atomi százalékban tartalmaztak. A mosatlan minták elemtérképei alapján a gipsz a $Mg(OH)_2$ felületén vált ki. A kinetikai mérések és a szilárd minták vizsgálatával kapott eredmények alapján azt mondhatjuk, hogy a csapadékok kiválásának *in situ* elválasztása megfelelő tervezés mellett lehetséges, és ígéretes koncepciót nyújt savas szennyvizek kezelésének környezeti és gazdaságossági szempontból való

fejlesztésére, valamint hasznosnak bizonyulhat tengervizet használó ipari folyamatokban, mint például sótalanítási eljárások során.

Annak érdekében, hogy meghatározzuk, hol található citrát a reakciók teljes lejátszódása után, HPLC segítségével megvizsgáltuk a reakcióból származó folyadék (szűrlet + mosófolyadék) és feloldott szilárd mintákat ($Mg(OH)_2$ és $CaSO_4 \cdot 2H_2O$). Az eredmények alapján a citrát egy része a $Mg(OH)_2$-hoz kötődik, míg másik része a folyadékfázisban marad, és akadályozza a gipsz kristályosodását. A szilárd minták IR spektrumai megerősítették ezeket az eredményeket. A citrát jelenlétében leválasztott $Mg(OH)_2$ spektrumán a magnézium-, illetve kalcium-citrátra jellemző sávokat azonosítottunk, míg a külön leválasztott gipszminták spektrumainak egyikén sem láthatunk szerves szennyezőre utaló jeleket. Az eredmények alapján azt feltételezzük, hogy a citrát egy része a $Mg(OH)_2$ felületére kötődik, és amennyiben szükséges, kalciumionok is megkötődhetnek, hogy kompenzálják a citrát-ionok töltését. Ezek alapján mind a szűrlet, mind pedig a $Mg(OH)_2$ újrafelhasználható a savas szennyvizek semlegesítése során, tovább javítva a folyamat gazdaságosságát és csökkentve a környezeti terhelést.

Acknowledgements

First, I need to express my gratitude to my supervisors, Dr. Pál Sipos and Dr. István Pálinkó, who provided me the opportunity to work in their research group since 2013, and always found time to help me through the bumps on the road. I also wish to thank Dr. Gábor Peintler for the immense and detailed work on the kinetics.

Many thanks for Chris du Plessis and Lhoist for the financial and material support and for the industrial and environmental insights.

I must express my gratitude also for Dr. Zoltán Kónya and Dr. Ákos Kukovecz for giving us the opportunity to use many of the measuring equipment.

I am grateful to Miklós Csáti for the ICP measurements, to Máté Náfrádi for the HPLC measurements, Ilona Halasiné Varga for the help during the laboratory work and to every member of the Materials and Solution Structure Research group who helped me during my work.

Many thanks to my family and friends, for always supporting me in hard times.

Finally, I wish to thank my girlfriend, Adél, for the emotional support, the constant motivation and encouragement.